Calcolo (2024) 61:65
https://doi.org/10.1007/s10092-024-00617-w

Stokes flow with Tresca boundary condition: a posteriori error analysis

R. Agroum[1] · J. K. Djoko[2] · J. Koko[3] · T. Sayah[4]

Received: 7 November 2023 / Revised: 6 August 2024 / Accepted: 21 September 2024 /
Published online: 8 October 2024
© The Author(s) under exclusive licence to Istituto di Informatica e Telematica (IIT) 2024

Abstract

In this article, a reliable a posteriori error estimate of residual type is derived for a variational inequality of second kind modeling Stokes equations with Tresca's boundary condition. Two sources of the error are considered here; the discretization error and the linearization error. Balancing these two errors is crucial to design an adaptive strategy for mesh refinement. Numerical results are reported to illustrate the good performance of the estimator constructed.

Keywords Stokes equations · Nonlinear slip boundary conditions · Variational inequality · Iterative solution · Estimator

Mathematics Subject Classification 65N30 · 76D07 · 35J85

Dedicated to the memory of Christine Bernardi (1955–2018).

✉ J. K. Djoko
jules.djokokamdem@gmail.com

R. Agroum
rahmaagroum@gmail.com

J. Koko
jonas.koko@uca.fr

T. Sayah
toni.sayah@usj.edu.lb

1 1EPF, Ecole d'Ingénieurs, 2 rue Fernand Sastre, 10430 Rosières-près-Troyes, France

2 School of Mathematical Sciences, North West University, Potchefstroom, South Africa

3 LIMOS, Université Clermont-Auvergne–CNRS UMR 6158, B.P 10448, 63000 Clermont-Ferrand, France

4 Laboratoire de Mathematiques et Applications, Unite de recherche "Mathematiques et Modelisation", Faculté des Sciences, Université Saint-Joseph, B.P 11-514, Riad El Solh, Beirut 1107 2050, Lebanon

1 Introduction

1.1 Governing equations

Let $\Omega \subset \mathbb{R}^2$ be a bounded domain and denote by $\partial\Omega$ its boundary, assumed to be Lipschitz-continuous. We consider the steady incompressible Stokes equations modeled by the system of equations

$$-2\nu div\, D\boldsymbol{u} + \nabla p = \boldsymbol{f} \quad \text{in } \Omega, \tag{1.1}$$

$$div\, \boldsymbol{u} = 0 \quad \text{in } \Omega\,, \tag{1.2}$$

where $\boldsymbol{u} = (u_i)_{i=1}^2$ is the velocity of fluid, p is the pressure of the fluid and $\boldsymbol{f}$ is the external body force applied to the fluid, ν is the kinematic viscosity and $D\boldsymbol{u} = 1/2\left(\nabla\boldsymbol{u} + (\nabla\boldsymbol{u})^\top\right)$ is the symmetric part of the velocity gradient. These Eqs. (1.1) and (1.2) are complemented by boundary conditions that are described next. For that purpose, we assume that $\partial\Omega$ is a union of two non-overlapping parts, that is $\partial\Omega = \overline{S}\cup\overline{\Gamma}$, with $S \cap \Gamma = \emptyset$, where S and Γ are relatively nonempty open subsets of $\partial\Omega$. Γ is subject to the adhesive boundary condition, that is

$$\boldsymbol{u} = \boldsymbol{0} \quad \text{on } \Gamma\,, \tag{1.3}$$

whereas on S, we assume the impermeability condition

$$\boldsymbol{u}\cdot\boldsymbol{n} = 0 \ \text{ on } \ S, \tag{1.4}$$

where $\boldsymbol{n} : S \longrightarrow \mathbb{R}^2$ is the normal outward unit vector to S. Thus S is an impermeable solid surface along which the fluid may slip. The orthogonal vector to $\boldsymbol{n}$ is denoted $\boldsymbol{\tau}$ and is called the tangential vector. The velocity along S is decomposed as follows

$$\boldsymbol{u} = (\boldsymbol{u}\cdot\boldsymbol{n})\boldsymbol{n} + (\boldsymbol{u}\cdot\boldsymbol{\tau})\boldsymbol{\tau} = \boldsymbol{u_n} + \boldsymbol{u_\tau}.$$

The force within the fluid is the Cauchy stress tensor $\boldsymbol{T}$ given by the relation

$$\boldsymbol{T} = 2\nu D\boldsymbol{u} - p\boldsymbol{I} \text{ on } \Omega,$$

where $\boldsymbol{I}$ is identity matrix in 2d. The traction force acting on S is $\boldsymbol{Tn}$. Similarly we have the following decomposition

$$\boldsymbol{Tn} = (\boldsymbol{Tn}\cdot\boldsymbol{n})\boldsymbol{n} + (\boldsymbol{Tn}\cdot\boldsymbol{\tau})\boldsymbol{\tau} = (\boldsymbol{Tn})_{\boldsymbol{n}} + (\boldsymbol{Tn})_{\boldsymbol{\tau}}.$$

Taking first the scalar product of $\boldsymbol{u}$ and the balance of linear momentum (1.1) and next employing the Green formula, (1.2) (1.3) and (1.4) we obtain

$$2\nu\int_\Omega |D\boldsymbol{u}|^2 dx + \int_S (-\boldsymbol{Tn})_{\boldsymbol{\tau}}\cdot\boldsymbol{u_\tau} d\sigma = \int_\Omega \boldsymbol{f}\cdot\boldsymbol{u} dx,$$

with $d\sigma$ being the surface measure associated to S. We note that $2\nu \int_\Omega |D\boldsymbol{u}|^2 dx$ is the dissipative energy mechanisms in the bulk, while the non-negative expression $\int_S (-\boldsymbol{Tn})_{\boldsymbol{\tau}} \cdot \boldsymbol{u}_{\boldsymbol{\tau}} d\sigma$ is the dissipative energy on the boundary S. It is manifest that to describe the fluid on S, we need a functional relation between $(\boldsymbol{Tn})_{\boldsymbol{\tau}}$ and $\boldsymbol{u}_{\boldsymbol{\tau}}$. We note that if $(\boldsymbol{Tn})_{\boldsymbol{\tau}}$ is zero, then one obtains the perfect slip boundary condition, while if the tangential velocity is zero, then one gets no-slip boundary condition. On the other hand, if the tangential component is expressed in the form $(\boldsymbol{Tn})_{\boldsymbol{\tau}} + \alpha \boldsymbol{u}_{\boldsymbol{\tau}} = \boldsymbol{0}$, with $\alpha \geq 0$, then one gets Navier's slip boundary condition. In this text, we are interested in threshold-slip (or stick–slip) boundary condition. Thus, let $g : S \longrightarrow [0, \infty)$ be a non-negative function called the threshold slip or the barrier function. The stick–slip boundary condition considered in this work was formulated by Fujita [1, 2] and reads as follows:

$$\left.\begin{aligned} &\text{If} \quad |(\boldsymbol{Tn})_{\boldsymbol{\tau}}| < g \Rightarrow \boldsymbol{u}_{\boldsymbol{\tau}} = \boldsymbol{0}, \\ &\text{If} \quad |(\boldsymbol{Tn})_{\boldsymbol{\tau}}| = g \Rightarrow \boldsymbol{u}_{\boldsymbol{\tau}} \neq \boldsymbol{0}\,, \ \text{and} \ \ -(\boldsymbol{Tn})_{\boldsymbol{\tau}} = g \frac{\boldsymbol{u}_{\boldsymbol{\tau}}}{|\boldsymbol{u}_{\boldsymbol{\tau}}|} \end{aligned}\right\} \ \text{on} \quad S\,, \tag{1.5}$$

where $|\boldsymbol{v}|^2 = \boldsymbol{v} \cdot \boldsymbol{v}$ is the Euclidean norm. We note that $\int_S (-\boldsymbol{Tn})_{\boldsymbol{\tau}} \cdot \boldsymbol{u}_{\boldsymbol{\tau}} d\sigma = \int_S g\, |\boldsymbol{u}_{\boldsymbol{\tau}}|\, d\sigma$ is positive. The stick–slip law (1.5) differs from the one formulated by Le Roux [3], which reads

$$\begin{aligned} &\text{If} \quad |(\boldsymbol{Tn})_{\boldsymbol{\tau}}| > g, \ \text{then slip occurs and} \ (\boldsymbol{Tn})_{\boldsymbol{\tau}} = -(g + \kappa |\boldsymbol{u}_{\boldsymbol{\tau}}|) \frac{\boldsymbol{u}_{\boldsymbol{\tau}}}{|\boldsymbol{u}_{\boldsymbol{\tau}}|} \\ &\text{If} \ |(\boldsymbol{Tn})_{\boldsymbol{\tau}}| \leq g \ \text{then no slip and} \ \boldsymbol{u}_{\boldsymbol{\tau}} = \boldsymbol{0}. \end{aligned} \tag{1.6}$$

The relation (1.6) can be re-written equivalently as follows

$$\boldsymbol{u}_{\boldsymbol{\tau}} = -\frac{1}{\kappa} \frac{\Big(|(\boldsymbol{Tn})_{\boldsymbol{\tau}}| - g\Big)^+}{|(\boldsymbol{Tn})_{\boldsymbol{\tau}}|} (\boldsymbol{Tn})_{\boldsymbol{\tau}} \tag{1.7}$$

with κ and g positive quantities and $a^+ = \max(a, 0)$ for $a \in \mathbb{R}$. One notes from (1.7) that if $g = 0$ then one gets the Navier's slip, but when $g > 0$, $(\boldsymbol{Tn})_{\boldsymbol{\tau}}$ cannot be considered as a function of $\boldsymbol{u}_{\boldsymbol{\tau}}$. We note that in abstract format some constitutive relations between $\boldsymbol{u}_{\boldsymbol{\tau}}$ and $(\boldsymbol{Tn})_{\boldsymbol{\tau}}$ leads to the implicit relation (see [4])

$$\psi(\boldsymbol{u}_{\boldsymbol{\tau}}, (\boldsymbol{Tn})_{\boldsymbol{\tau}}) = 0 \tag{1.8}$$

where ψ may not be a function (can be multi valued). The possibility that (1.5) can be written in the form (1.8) is not known to the authors. Problems with threshold-slip (or stick–slip) boundary condition are of great interest since the processes involving stick–slip between two entities occurs in many engineering and industrial applications. We refer to [5, 6] for modeling and detailed understanding of contact and friction in

solid mechanics. In fluid mechanics, the friction boundary condition was introduced by Fujita [1, 2] and later on, Le Roux in [3] has formulated a friction condition given rise to a family quasi-variational inequalities. A rigorous mathematical study of these problems within the framework of variational inequalities is presented in [7], while a comprehensive numerical analysis of variational inequalities is treated in [8], we also note the early (important) contributions presented in [9–11]. Before presenting the main goal of this work, we recall that the continuous problem has been treated in [1, 2, 12], while a similar abstract problem has been analysed in [13, 14]. A weak form of the partial differential equations (1.1), (1.2), (1.3), (1.4) and (1.5) reads:

$$\begin{cases} \text{Find } (\boldsymbol{u}, p) \in \mathbb{V} \times M, \text{ such that for all } (\boldsymbol{v}, q) \in \mathbb{V} \times M, \\ a(\boldsymbol{u}, \boldsymbol{v}-\boldsymbol{u}) + b(\boldsymbol{v}-\boldsymbol{u}, p) + j(\boldsymbol{v}) - j(\boldsymbol{u}) \geq \ell(\boldsymbol{v}-\boldsymbol{u}), \\ b(\boldsymbol{u}, q) = 0, \end{cases} \tag{1.9}$$

with $\mathbb{V} = \left\{ \boldsymbol{v} \in \left[H^1(\Omega)\right]^2 : \boldsymbol{v}|_\Gamma = 0 \ , \ \boldsymbol{v} \cdot \boldsymbol{n}|_S = 0 \right\}$, $M = L^2_0 = \left\{ p \in L^2(\Omega) : \int_\Omega p dx = 0 \right\}$ and

$$\begin{aligned} a(\boldsymbol{u}, \boldsymbol{v}) &= 2\nu \int_\Omega D\boldsymbol{u} : D\boldsymbol{v} dx, \quad b(\boldsymbol{v}, q) = -\int_\Omega div\, \boldsymbol{v} q dx \\ \ell(\boldsymbol{v}) &= \int_\Omega \boldsymbol{f} \cdot \boldsymbol{v} dx, \quad j(\boldsymbol{v}) = \int_S g|\boldsymbol{v}_{\boldsymbol{\tau}}| d\sigma. \end{aligned}$$

We recall that $H^k(\Omega)$ and $\|\cdot\|_k$ denote the standard Sobolev space and its norm, $L^2(\Omega)$ and $\|\cdot\|$ the standard Lebesgue space and its norm (see [15] for more details), and $\boldsymbol{A} : \boldsymbol{B} = \sum_{1 \leq i,j \leq 2} A_{ij} B_{ij}$ with $\boldsymbol{A} = (A_{ij})$ and $\boldsymbol{B} = (B_{ij})$. We next characterize the solution $(\boldsymbol{u}, p)$ of (1.9) through the use of a Lagrange field (not exactly of Lagrange's type) which is more suitable for numerical computations (see [16, 17]).

Lemma 1.1 *There exists a unique* $\boldsymbol{\alpha} \in \left[L^2(S)\right]^2$ *with* $|\boldsymbol{\alpha}| \leq 1$ *such that* $(\boldsymbol{u}, p)$ *solves* (1.9) *if and only if*

$$\begin{cases} a(\boldsymbol{u}, \boldsymbol{v}) + b(\boldsymbol{v}, p) + \int_S g\boldsymbol{\alpha} \cdot \boldsymbol{v}_{\boldsymbol{\tau}} d\sigma = \ell(\boldsymbol{v}) \text{ for all } \boldsymbol{v} \in \mathbb{V}, \\ b(\boldsymbol{u}, q) = 0 \text{ for all } q \in M, \\ \boldsymbol{\alpha} \cdot \boldsymbol{u}_{\boldsymbol{\tau}} = |\boldsymbol{u}_{\boldsymbol{\tau}}| \text{ a.e on } S. \end{cases} \tag{1.10}$$

We note that one of the difficulties when implementing (1.10) is the verification of the third equation in (1.10), which is equivalent to the following statements:

$$\begin{aligned} &1. \quad \int_S \boldsymbol{u}_{\boldsymbol{\tau}} \cdot (\boldsymbol{\alpha} - \boldsymbol{\mu}) d\sigma \geq 0 \quad \text{for all } \boldsymbol{\mu} \in \Lambda \\ &2. \quad \boldsymbol{\alpha} = P_\Lambda (\boldsymbol{\alpha} + \boldsymbol{u}_{\boldsymbol{\tau}}). \end{aligned} \tag{1.11}$$

In (1.11), Λ is a closed convex subset of $\left[L^2(S)\right]^2$ (or $\left[L^\infty(S)\right]^2$ actually) defined by

$$\Lambda = \left\{ \boldsymbol{\alpha} \in \left[L^2(S)\right]^2 : \ |\boldsymbol{\alpha}| \leq 1 \text{ a.e. on } S \right\},$$

and P_Λ is the orthogonal projection operator from $\left[L^2(S)\right]^2$ onto Λ given as follows

$$P_\Lambda(\boldsymbol{\alpha}) = \frac{\boldsymbol{\alpha}}{\sup(1, |\boldsymbol{\alpha}|)}. \tag{1.12}$$

It is then manifest that an iterative scheme can be easily formulated using the second relation in (1.11), but the drawback here is that we will have a severe restriction on the velocity. Thus in order to avoid a condition on the velocity, we note that since g is non-negative, the third relation in (1.10) is also equivalent to the following statements:

$$\begin{aligned} &1. \quad \int_S g\boldsymbol{u_\tau} \cdot (\boldsymbol{\alpha} - \boldsymbol{\mu}) d\sigma \geq 0 \quad \text{for all } \boldsymbol{\mu} \in \Lambda, \\ &2. \quad \boldsymbol{\alpha} = P_\Lambda\left(\boldsymbol{\alpha} + g\rho\boldsymbol{u_\tau}\right) \qquad \text{for all } \rho > 0, \end{aligned} \tag{1.13}$$

ρ being a relaxation parameter that will be chosen later to ensure the convergence of the iterative scheme (see (2.10)). An important property that will be needed in this text is the following (see [16, P. 89, Lemma 6.1])

Lemma 1.2 *P_Λ is a contraction, that is*

$$\text{for all } \boldsymbol{\alpha}, \boldsymbol{\beta} \in \left[L^2(S)\right]^2, \ \|P_\Lambda(\boldsymbol{\alpha}) - P_\Lambda(\boldsymbol{\beta})\|_S \leq \|\boldsymbol{\alpha} - \boldsymbol{\beta}\|_S.$$

With the introduction of the operator P_Λ and having in mind the second relation in (1.13), we note that the variational problem (1.10) is equivalent to

$$\begin{cases} a(\boldsymbol{u}, \boldsymbol{v}) + b(\boldsymbol{v}, p) + \displaystyle\int_S g\boldsymbol{\alpha} \cdot \boldsymbol{v_\tau} d\sigma = \ell(\boldsymbol{v}) \text{ for all } \boldsymbol{v} \in \mathbb{V}, \\ b(\boldsymbol{u}, q) = 0 \text{ for all } q \in M, \\ \boldsymbol{\alpha} = P_\Lambda\left(\boldsymbol{\alpha} + \rho g \boldsymbol{u_\tau}\right) \text{ a.e. on } S, \text{ for all } \rho > 0. \end{cases} \tag{1.14}$$

The goal of this work is to propose residual based a posteriori error analysis of (1.9) taking into account the discretization scheme and the linearization of the nonlinear system of equations to be solved.

1.2 A posteriori estimators for variational inequalities

The literature on numerical analysis of variational inequalities is rich and dated back to the early seventies at least (see [9–11] just to cite a few). The variational problem (1.9) has been solved numerically with finite element approximation by many authors (see

[18–25]). A residual based a posteriori error analysis for elliptic variational inequalities is addressed in [26–40], while some abstract a posteriori error analyses for variational inequalities of first and second kind with Lagrange field are presented in [41–43]. The equilibrated flux reconstruction approach has also been used to analyse the a posteriori error for elliptic variational inequalities with some success in [44–50]. We note that the first studies on a posteriori error estimators (with a residual based approach) for Stokes equations with Tresca's boundary condition has been proposed by W. Han and co-authors in [38, 39] for conforming and discontinuous Galerkin schemes. In their studies, reliable and efficient estimators are constructed. The error in the Lagrange field, which is part of the solution is also controlled. Moreover, adaptive mesh refinement strategy is proposed and numerical simulations confirming the theoretical results are shown. In [40], Bingham flow is considered in a cylindrical pipe. A priori and a posteriori error analysis is presented taking into account the Lagrange field. We emphasize that, the main ingredient in that work is the introduction of a discrete mesh dependent norm for the normalized Lagrange field which allows proving stability for many finite elements. We note that iterative adaptive mesh refinement is not discussed in [38–40]. In [49, 50] iterative adaptive algorithms for variational inequalities of first kind is considered for conforming and non-conforming schemes using Newton's iteration method. An equilibrated flux reconstruction a posteriori error estimator that ensures guaranteed upper bound on the energy error between the continuous solution and the discrete solution at any resolution step is presented.

A principal result in our paper is the construction of the reliable residual-based a posteriori error estimator for the variational problem (1.9) taking into account both the discretization and the iterative error. This problem has not yet been treated. We quickly note that the main difficulties in our analysis are: the presence of inequality symbol (due to the Trecsa's boundary condition) and the error committed in the resolution of the resulting nonlinear system of equations. In this paper, we derive residual a posteriori error estimates for the velocity and pressure, and show that the estimator is reliable, that is, it provides an upper bound of the error in the natural variational norm. A key step in our analysis is the use of a Lagrange field which formally turns the inequality into an equation. Thus, an Uzawa scheme is formulated with the help of a projection operator, whose properties are then used to construct the estimator and establish its reliability (see details in Sect. 3, Theorem 3.1). We split the estimator into space and "linearization" parts. The indicator due to the discretization is similar to the ones we know for the Stokes equations (the only difference being the contribution of the tangential stress which is acting on S), while the indicator due to the linearization although not easily inferred from the equations is pretty reasonable because on S we have a nonlinear and not differentiable expression. Hence the linearization should occur on the boundary S. We report in Remark 3.2 on our attempt to establish the efficiency of the indicator. We shall see that this leads to some difficult issues, indicating that our work in this project is not yet complete.

The computable upper error bound leads to a criterion for automatic mesh-refinements within a finite element method. As mentioned before, we have separated the estimator into two parts: the part being coming from the error of the numerical discretization of the weak formulation (1.9) (or (1.10)), and the second part comes from the resolution of the nonlinear problem (2.9). Thus the idea in the adaptive mesh

strategy is to use these contributions to reduce the computations and achieve good refinement. We note that, if the discretization error dominates then the number of iterations of the solver is reduced. It is worth noticing that this type of analysis was introduced by Chaillou and Suri [51, 52] for a class of problems with a strongly monotone operator, and extended later on in [53]. These results have been further developed in [54–56].

1.3 Outline of the paper

The paper is organized as follows. In Sect. 2, we introduce the variational formulation related to the Stokes equations with Tresca's boundary condition. Then we present known results on finite element approximations and iterative schemes. We provide a posteriori error analysis for the scheme in Sect. 3. This is the key theoretical contribution on this work. We construct an indicator consisting of two sub quantities namely; (i) the discretization term and (ii) the linearization term. We prove that the actual error is less than the indicator. In Sect. 4, we present some numerical examples that validate the theoretical findings.

2 Preliminaries

This section introduces some classical inequalities that will be used later in the text. We also introduce some useful notation about the discrete setting and the *a priori* error analysis. Finally, we formulate an iterative algorithm for the practical resolution of the nonlinear finite element problem.

The following Sobolev imbedding will be used: for any real number $p \geq 1$, there exists a positive constant c_p^0 such that (see [15, Chap 7])

$$\text{for all } \boldsymbol{v} \in \mathbb{V}\,, \quad \|\boldsymbol{v}\|_{L^p(\Omega)}^2 \leq c_p^0 \|\nabla \boldsymbol{v}\|^2 = c_p^0 \int_\Omega |\nabla \boldsymbol{v}|^2 \, dx\,. \tag{2.1}$$

Noting that (2.1) is Poincaré's inequality when $p = 2$. Of importance also is the Korn's inequality which reads (see [6, Chap 4])

$$\text{for all } \boldsymbol{v} \in \mathbb{V}\,, \quad \int_\Omega |\nabla \boldsymbol{v}|^2 \, dx \leq c \int_\Omega |D\boldsymbol{v}|^2 \, dx. \tag{2.2}$$

2.1 The finite element method

We introduce here some notations about the finite element discretization, and state important results about the convergence of the discrete solution.

From now on, we assume that Ω is a polygon. Hence $\overline{\Omega}$ can be completely meshed. We denote by $\mathcal{T}_h$ the regular family of triangulations of Ω, in the sense that (see [57])), for each $h > 0$:

- The union of all elements of $\mathcal{T}_h$ is equal to $\overline{\Omega}$;

- The intersection of two different elements of $\mathcal{T}_h$ is either empty, a common vertex or an entire common edge;
- The ratio of the diameter h_K of an element K of $\mathcal{T}_h$ to the diameter of its inscribed circle is smaller than a constant independent of h.

As usual h denotes the maximal diameter h_K, when $K \in \mathcal{T}_h$. For each $K \in \mathcal{T}_h$, and for each nonnegative integer k, $\mathcal{P}_k(K)$ is the space of restrictions to K of polynomials with 2 variables with degree less than or equal to k.
In what follows, c stands for a generic constant which may vary from line to line but is always independent of h. The velocity and pressure are approximate by using conforming finite dimensional spaces $\mathbb{V}_h$ and M_h respectively given by

$$\mathbb{V}_h = \left\{ \boldsymbol{v}_h \in \mathbb{V} \cap \left[\mathcal{C}(\overline{\Omega})\right]^2, \text{ for all } K \in \mathcal{T}_h, \ \ \boldsymbol{v}_h|_K \in [\mathcal{P}_1(K) + \text{"bubble"}]^2 \right\}, \tag{2.3}$$

where $\mathcal{P}_1(K)$+"bubble" is the sum of a polynomial of $\mathcal{P}_1(K)$ and a "bubble" function $b_K(\boldsymbol{x}) = \alpha_1(\boldsymbol{x})\alpha_2(\boldsymbol{x})\alpha_3(\boldsymbol{x})$, for any $K \in \mathcal{T}_h$, and denoting the vertices of $K \in \mathcal{T}_h$ by a_i, $1 \leq i \leq 3$, and its corresponding barycentric coordinates by α_i. Note that $b_K(\boldsymbol{x}) = 0$ on ∂K and that $b_K(\boldsymbol{x}) > 0$ in the interior of K. The pressure is approximated in the space M_h given as follows

$$M_h = \left\{ q_h \in M \cap \mathcal{C}(\overline{\Omega}), \ \ \text{for all } K \in \mathcal{T}_h, \ \ q_h|_K \in \mathcal{P}_1(K) \right\}. \tag{2.4}$$

We are well aware that the spaces $\mathbb{V}_h$ and M_h are inf-sup stable in the following sense (see [58]): there exists $\beta > 0$ (independent of h) such that

$$\text{for all} \quad p_h \in M_h \quad \beta \|p_h\| \leq \sup_{\boldsymbol{v} \in \mathbb{V}_h} \frac{b(\boldsymbol{v}, p_h)}{\|\boldsymbol{v}\|_1}. \tag{2.5}$$

With these preliminaries in place, we approximate (1.9) by the following finite element scheme

$$\begin{cases} \text{Find } \ (\boldsymbol{u}_h, p_h) \in \mathbb{V}_h \times M_h, \ \ \text{such that for all } \ (\boldsymbol{v}, q) \in \mathbb{V}_h \times M_h, \\ a(\boldsymbol{u}_h, \boldsymbol{v} - \boldsymbol{u}_h) + b(\boldsymbol{v} - \boldsymbol{u}_h, p_h) + j(\boldsymbol{v}) - j(\boldsymbol{u}_h) \geq \ell(\boldsymbol{v} - \boldsymbol{u}_h), \\ b(\boldsymbol{u}_h, q) = 0. \end{cases} \tag{2.6}$$

The discrete problem (2.6) has a unique solution $(\boldsymbol{u}_h, p_h) \in \mathbb{V}_h \times M_h$ (see [18, 20, 22–24]) which satisfies

$$\|\boldsymbol{u}_h\|_1 + \|p_h\| \leq c\|\boldsymbol{f}\| + c\|g\|_{L^\infty(S)},$$

moreover we have

$$\|\boldsymbol{u} - \boldsymbol{u}_h\|_1 + \|p - p_h\| \leq c \inf_{v_h \in \mathbb{V}_h} \|\boldsymbol{u} - \boldsymbol{v}_h\|_1 + c \inf_{q_h \in M_h} \|p - q_h\| + c \inf_{v_h \in \mathbb{V}_h} \|\boldsymbol{u} - \boldsymbol{v}_h\|_S^{1/2}. \tag{2.7}$$

Remark 2.1 Assuming the regularity $(\boldsymbol{u}, p) \in \left[H^2(\Omega)\right]^2 \times H^1(\Omega)$, which is not guaranteed in general, we take $(\boldsymbol{v}_h, q_h) = (I_h \boldsymbol{u}, \Pi_h p)$ with I_h being the Lagrange interpolation and Π_h a local regularization operator. Then (2.7) implies that

$$\|\boldsymbol{u} - \boldsymbol{u}_h\|_1 + \|p - p_h\| \leq ch^{3/4} .$$

But if one takes $\boldsymbol{u}_{\boldsymbol{\tau}} \in \left[H^2(S)\right]^2$, then

$$\|\boldsymbol{u} - \boldsymbol{u}_h\|_1 + \|p - p_h\| \leq ch .$$

Thus the rate of convergence is dominated by the interpolation estimate on the slip zone. So, the regularity of the tangential velocity on the slip zone will determine the rate of convergence of the finite element method. We also note that the rate of convergence of order one can be obtained if one replaces j by j_h, with j_h being an approximation of j obtained by the trapezoidal rule (see [8, 16, 23]). It is worth noting that the results presented so far are also valid in 3d.

Analogous to Lemma 1.1, the solution $(\boldsymbol{u}_h, p_h)$ of the discrete problem (2.6) can be characterized by the following result (see [36, Theorem 3.1])

Lemma 2.1 *There exists a unique* $\boldsymbol{\alpha}_h \in \Lambda$ *such that* $(\boldsymbol{u}_h, p_h)$ *solves* (2.6) *if and only if*

$$\begin{cases} a(\boldsymbol{u}_h, \boldsymbol{v}_h) + b(\boldsymbol{v}_h, p_h) + \displaystyle\int_S g\boldsymbol{\alpha}_h \cdot \boldsymbol{v}_{\boldsymbol{\tau}h} d\sigma = \ell(\boldsymbol{v}_h) \text{ for all } \boldsymbol{v}_h \in \mathbb{V}_h , \\ b(\boldsymbol{u}_h, q_h) = 0 \text{ for all } q_h \in M_h , \\ \boldsymbol{\alpha}_h \cdot \boldsymbol{u}_{\boldsymbol{\tau}h} = |\boldsymbol{u}_{\boldsymbol{\tau}h}| \text{ on } S. \end{cases} \tag{2.8}$$

We note from the projection theorem that the third relation in (2.8) can be re-written as follows

$$\boldsymbol{\alpha}_h = P_\Lambda \left(\boldsymbol{\alpha}_h + \rho g \boldsymbol{u}_{\boldsymbol{\tau}h}\right) \quad \text{on } S \text{ for all } \rho > 0.$$

2.2 Iterative scheme

Since the discrete problem (2.6) is nonlinear, it can only be solved by iterative or incremental methods. We note at this juncture that several methods are available in the literature for the practical resolution of (2.6) (see [20, 49, 50] just to cite a few). In this paper, we find the solution of (2.6) via the Uzawa's algorithm because the algorithm decouples the velocity and pressure from the Lagrange field. Hence, this approach requires the solution of the Stokes system in each "velocity/pressure" direction. Another advantage of this approach is that the Lagrange field is explicit in each iteration. So, the scheme is easy to implement. Also, we note that the convergence of the algorithm is guaranteed once the relaxation parameter is correctly taken irrespective of the starting point in Λ. However, if the initial guess is sufficiently close to the

theoretical solution, then the semismooth Newton, interior point method or active set approach lead to much faster convergence rates than the Uzawa iteration.

Owing to the equivalence between the problems (2.8) and (2.6), we propose next an iterative scheme for its resolution.

Uzawa algorithm. Let $\boldsymbol{\alpha}_h^0 \in \Lambda$ be an initial guess. For $n \geq 1$, $\boldsymbol{\alpha}_h^{n-1}$ being known, we compute $(\boldsymbol{u}_h^n, p_h^n)$ and $\boldsymbol{\alpha}_h^n$ as follows

$$\begin{cases} a(\boldsymbol{u}_h^n, \boldsymbol{v}) + b(\boldsymbol{v}, p_h^n) = -\displaystyle\int_S g\boldsymbol{\alpha}_h^{n-1} \cdot \boldsymbol{v}_{\boldsymbol{\tau}} d\sigma + \ell(\boldsymbol{v}) \text{ for all } \boldsymbol{v} \in \mathbb{V}_h \,, \\ b(\boldsymbol{u}_h^n, q) = 0 \text{ for all } q \in M_h \,, \\ \boldsymbol{\alpha}_h^n = P_\Lambda \left(\boldsymbol{\alpha}_h^{n-1} + \rho g \boldsymbol{u}_{\boldsymbol{\tau},h}^n \right) \,, \end{cases} \tag{2.9}$$

where ρ is a relaxation parameter, a positive constant chosen in such a way as to achieve convergence of the scheme, and P_Λ is the projection operator introduced before (see (1.12)). From the properties of $a(\cdot,\cdot)$ and $b(\cdot,\cdot)$, one verifies that the problem (2.9) has a unique solution that depends continuously on $(\boldsymbol{f}, g)$:

$$\|\boldsymbol{u}_h^n\|_1 + \|p_h^n\| \leq c \left(\|g\|_{L^\infty(S)} + \|\boldsymbol{f}\| \right) \,.$$

We note that at each iteration step, $\left|\boldsymbol{\alpha}_h^n\right| \leq 1$. The proof of the convergence of the algorithm (2.9) relies on the properties of $a(\cdot,\cdot)$, $b(\cdot,\cdot)$ and P_Λ. In fact we have

Theorem 2.1 *Let $(\boldsymbol{u}_h^n, p_h^n, \boldsymbol{\alpha}_h^n)$ be the solution of the problem (2.9), and $(\boldsymbol{u}_h, p_h, \boldsymbol{\alpha}_h)$ the solution of the problem (2.8). Then there exists a constant c independent of both h and n such that if*

$$0 < \rho \leq c\nu / \|g\|^2_{L^\infty(S)}, \tag{2.10}$$

then

$$\lim_n \|\boldsymbol{u}_h^n - \boldsymbol{u}_h\|_1 = 0, \quad \lim_n \|p_h^n - p_h\| = 0.$$

For the proof, we refer to [16, Theorem 6.9] where similar arguments are presented. □

The next result indicates the viability of the algorithm (2.9).

Lemma 2.2 *The algorithm (2.9) is consistent with (2.8) in the sense that if there exists $m \geq 1$ such that the solution $(\boldsymbol{\alpha}_h^m, \boldsymbol{u}_h^m, p_h^m)$ coincides with the solution $(\boldsymbol{\alpha}_h, \boldsymbol{u}_h, p_h)$ of (2.8), then for all $n > m$, $(\boldsymbol{\alpha}_h^n, \boldsymbol{u}_h^n, p_h^n)$ coincides with $(\boldsymbol{\alpha}_h, \boldsymbol{u}_h, p_h)$.*

Proof It is done by induction. We assume that up to $n-1$, the solutions of (2.9) and (2.8) are the same. We take the difference between (2.9) and (2.8) and obtain that

$$\begin{cases} a(\boldsymbol{u}_h^n - \boldsymbol{u}_h, \boldsymbol{v}) + b(\boldsymbol{v}, p_h^n - p_h) = 0 \quad \text{for all } \boldsymbol{v} \in \mathbb{V}_h, \\ b(\boldsymbol{u}_h^n - \boldsymbol{u}_h, q) = 0 \text{ for all } q \in M_h, \\ \boldsymbol{\alpha}_h^n - \boldsymbol{\alpha}_h = P_\Lambda \left(\boldsymbol{\alpha}_h + \rho g \boldsymbol{u}_{\boldsymbol{\tau}\, h}^n \right) - P_\Lambda \left(\boldsymbol{\alpha}_h + \rho g \boldsymbol{u}_{\boldsymbol{\tau}\, h} \right). \end{cases} \tag{2.11}$$

taking $\boldsymbol{v} = \boldsymbol{u}_h^n - \boldsymbol{u}_h$, and using the second relation in (2.11), we obtain $a(\boldsymbol{u}_h^n - \boldsymbol{u}_h, \boldsymbol{u}_h^n - \boldsymbol{u}_h) = 0$. Thus we deduce (using the coercivity of $a(\cdot,\cdot)$) that $\boldsymbol{u}_h^n = \boldsymbol{u}_h$, which implies $\boldsymbol{\alpha}_h = \boldsymbol{\alpha}_h^n$. The first relation in (2.11) is therefore reduced to $b(\boldsymbol{v}, p_h^n - p_h) = 0$. But the inf-sup condition (see (2.5)) leads to $p_h^n = p_h$. So the proof is complete. □

Remark 2.2 We note that this concept of consistency has been introduced in [59, Remark 5] when analysing a numerical solution of a Darcy–Forchheimer model with nonconforming elements.

We discuss next the main result of this work.

3 A posteriori error analysis

In this section, we construct a residual type a posteriori error estimate for the error $\|\boldsymbol{u} - \boldsymbol{u}_h^n\|_1 + \|p - p_h^n\|$ and examine its reliability. We also present the difficulties we encountered to establish the (local) efficiency of the a posteriori error estimate. We shall see that this leads to some difficult problems to solve.
In this section, C stands for a generic constant which may vary from line to line but is always independent of h, $(\boldsymbol{u}_h^n, p_h^n)$ and $(\boldsymbol{u}, p)$.

3.1 Preliminaries

We first introduce the standard notations which are needed for the derivation of error indicators later in the work. Thus, for an element $T \in \mathcal{T}_h$, $\mathcal{E}(T)$ is the set of its edges, while $\mathcal{N}(T)$ stands for the set of its vertices.

$$\mathcal{E}_h = \bigcup_{T\in\mathcal{T}_h} \mathcal{E}(T), \quad \mathcal{N}_h = \bigcup_{T\in\mathcal{T}_h} \mathcal{N}(T).$$

For any edge $e \in \mathcal{E}_h$, we associate a unit vector $\boldsymbol{n}_e$ orthogonal to e. We can split $\mathcal{E}_h$ as follows

$$\mathcal{E}_h = \mathcal{E}_{\Omega,h} \cup \mathcal{E}_{\Gamma,h} \cup \mathcal{E}_{S,h},$$

where $\mathcal{E}_{\Omega,h}$ is the set of interior edges, $\mathcal{E}_{\Gamma,h}$ is the set of edges that lie on Γ and $\mathcal{E}_{S,h}$ stands for the set of edges that lie on S. Following the same methodology one has

$$\mathcal{N}_h = \mathcal{N}_{\Omega,h} \cup \mathcal{N}_{\Gamma,h} \cup \mathcal{N}_{S,h}.$$

We recall that for $T \in \mathcal{T}_h$, and $e \in \mathcal{E}_h$, $|T|$ denote the area of T, h_T is the diameter of T while h_e is the length of e. To handle non smooth functions, we define the broken Sobolev space

$$\left[H^1(\Omega, \mathcal{T}_h)\right]^2 := \left\{\boldsymbol{v} \in \left[L^2(\Omega)\right]^2 : \quad \boldsymbol{v}|_K \in \left[H^1(K)\right]^2, \text{ for all } K \in \mathcal{T}_h\right\}.$$

We note that for each edge e, we associate a normal unit vector $\boldsymbol{n}_e$. If the edge e is on the boundary, the unit vector $\boldsymbol{n}_e$ is taken to be the outward normal to $\partial\Omega$. Let e_k be an edge shared by elements K_i and K_j with $\boldsymbol{n}_k$ pointing from K_i to K_j. The jump $[\cdot]_k$ and the mean value of $\{\cdot\}_k$ of a function v across e_k are given by

$$[v]_{e_k} = v|_{\partial K_i} - v|_{\partial K_j} \text{ and } \{v\}_{e_k} = \frac{1}{2}\left(v|_{\partial K_i} + v|_{\partial K_j}\right).$$

If $e = K_1 \cap \partial\Omega$, then the jump and average of v coincide with its trace on e.

The following integration by parts formula will be used in the subsequent analysis

$$\begin{aligned}
&\text{for all } (\boldsymbol{v}, \boldsymbol{T}) \in \left[H^1(\Omega, \mathcal{T}_h)\right]^2 \times \left[H^1(\Omega, \mathcal{T}_h)\right]^{2\times 2} \cap \{\boldsymbol{T} = \boldsymbol{T}^\top\},\\
&\int_\Omega \boldsymbol{T} : D\boldsymbol{v}dx + \int_\Omega div\, \boldsymbol{T} \cdot \boldsymbol{v}dx = \sum_{e\in\mathcal{E}_{\Omega,h}} \int_e [\boldsymbol{T}]\boldsymbol{n}_e \cdot \{\boldsymbol{v}\}d\sigma + \sum_{e\in\mathcal{E}_h} \int_e \{\boldsymbol{T}\}\boldsymbol{n}_e \cdot [\boldsymbol{v}]d\sigma.
\end{aligned} \tag{3.1}$$

An important tool in deriving the error indicator is Clément's operator $\mathcal{R}_h$ with values in $\mathbb{V}_h$. Thus, we start by considering the operator π_h introduces by Scott and Zhang (see [60]) that is quasi-locally stable in $L^2(\Omega)$. But it is obvious that π_h does not preserve the tangential character of the boundary data. Thus, we modify it as in [61, Section 5-2, 156–158]), and called the new operator $\mathcal{R}_h$ which by the way has the following local approximation properties (see Verfürth [62, Chap 1]):

$$\|\boldsymbol{v} - \mathcal{R}_h\boldsymbol{v}\|_K \leq ch_K\|\boldsymbol{v}\|_{1,\Delta_K}, \tag{3.2}$$

where Δ_K is the following set

$$\Delta_K = \bigcup \{K_1 \in \mathcal{T}_h : \ K_1 \cap K \neq \emptyset\} \ .$$

For the pressure, we shall used the interpolation operator $r_h : L^2_0(\Omega) \longrightarrow M_h$ described in [61, Section 5-2] and is given as follows:

$$\text{for all } (q, p) \in \mathcal{P}_1(K) \times L^2_0(\Omega), \quad \int_K q\,(r_h p - p)\,dx = 0 \quad \text{for all } K \in \mathcal{T}_h$$

and satisfies; for any real $s \in [0, 1]$

$$\text{for all } q \in H^s(\Omega) \cap L^2_0(\Omega), \quad \|r_h q - q\|_K \leq ch^s_K|q|_{H^s(K)}.$$

We denote by $\boldsymbol{f}_K$ and g_e the piecewise approximation of $\boldsymbol{f}$ and g respectively, such that in each element $K \in \mathcal{T}_h$ (respectively at each edge e on $\mathcal{E}_h$) we have:

$$\boldsymbol{f}_K = \frac{1}{|K|}\int_K \boldsymbol{f}(x)dx, \quad g_e = \frac{1}{|e|}\int_e g(x)d\sigma.$$

In order to get the useful estimators, we will write the residual equations considering (1.14) and (2.9). Let $(\boldsymbol{u}, p, \boldsymbol{\alpha})$ and $(\boldsymbol{u}^n, p_h^n, \boldsymbol{\alpha}_h^n)$ be the solution of (1.14) and (2.9) respectively. Then for $\boldsymbol{v} \in \mathbb{V}$ and $q \in M$, we have:

$$\begin{cases} a(\boldsymbol{u}-\boldsymbol{u}_h^n, \boldsymbol{v}) + b(\boldsymbol{v}, p-p_h^n) + \int_S g\boldsymbol{\alpha}\cdot\boldsymbol{v}_{\boldsymbol{\tau}} d\sigma = \int_\Omega \boldsymbol{f}\cdot\boldsymbol{v} dx - a(\boldsymbol{u}_h^n, \boldsymbol{v}) - b(\boldsymbol{v}, p_h^n) \\ b(\boldsymbol{u}-\boldsymbol{u}_h^n, q) = -b(\boldsymbol{u}_h^n, q). \end{cases} \tag{3.3}$$

For any $\boldsymbol{v}_h \in \mathbb{V}_h$, and having in mind (2.9), we have

$$\begin{aligned} \int_\Omega \boldsymbol{f}\cdot\boldsymbol{v} dx &= \int_\Omega \boldsymbol{f}\cdot(\boldsymbol{v}-\boldsymbol{v}_h) dx + \int_\Omega \boldsymbol{f}\cdot\boldsymbol{v}_h dx \\ &= \int_\Omega \boldsymbol{f}\cdot(\boldsymbol{v}-\boldsymbol{v}_h) dx + a(\boldsymbol{u}_h^n, \boldsymbol{v}_h) + b(\boldsymbol{v}_h, p_h^n) + \int_S g\boldsymbol{\alpha}_h^{n-1}\cdot\boldsymbol{v}_{\boldsymbol{\tau}h} d\sigma, \end{aligned}$$

which together with (3.3) gives

$$\begin{cases} a(\boldsymbol{u}-\boldsymbol{u}_h^n, \boldsymbol{v}) + b(\boldsymbol{v}, p-p_h^n) = \int_\Omega \boldsymbol{f}\cdot(\boldsymbol{v}-\boldsymbol{v}_h) dx - a(\boldsymbol{u}_h^n, \boldsymbol{v}-\boldsymbol{v}_h) - b(\boldsymbol{v}-\boldsymbol{v}_h, p_h^n) \\ \qquad\qquad + \int_S g\boldsymbol{\alpha}_h^{n-1}\cdot\boldsymbol{v}_{\boldsymbol{\tau}h} d\sigma - \int_S g\boldsymbol{\alpha}\cdot\boldsymbol{v}_{\boldsymbol{\tau}} d\sigma \\ b(\boldsymbol{u}-\boldsymbol{u}_h^n, q) = -b(\boldsymbol{u}_h^n, q)\,. \end{cases}$$

Here and henceforth, we take $\boldsymbol{T}_h^n = 2\nu D\boldsymbol{u}_h^n - p_h^n \boldsymbol{I}$. We apply (3.1) in each triangle K and obtain the following relation

$$\begin{cases} a(\boldsymbol{u}-\boldsymbol{u}_h^n, \boldsymbol{v}) + b(\boldsymbol{v}, p-p_h^n) = \int_\Omega \boldsymbol{f}\cdot(\boldsymbol{v}-\boldsymbol{v}_h) dx + \sum_{K\in\mathcal{T}_h}\int_K \div \boldsymbol{T}_h^n\cdot(\boldsymbol{v}-\boldsymbol{v}_h) dx \\ \quad - \sum_{e\in\mathcal{E}_{\Omega,h}}\int_e [\boldsymbol{T}_h^n]\boldsymbol{n}_e\cdot\{\boldsymbol{v}-\boldsymbol{v}_h\} d\sigma - \sum_{e\in\mathcal{E}_h}\int_e \{\boldsymbol{T}_h^n\}\boldsymbol{n}_e\cdot[\boldsymbol{v}-\boldsymbol{v}_h] d\sigma \\ \quad + \int_S g\boldsymbol{\alpha}_h^{n-1}\cdot\boldsymbol{v}_{\boldsymbol{\tau}h} d\sigma - \int_S g\boldsymbol{\alpha}\cdot\boldsymbol{v}_{\boldsymbol{\tau}} d\sigma \\ b(\boldsymbol{u}-\boldsymbol{u}_h^n, q) = -b(\boldsymbol{u}_h^n, q)\,. \end{cases} \tag{3.4}$$

$\boldsymbol{v} \in \left[H^1(\Omega)\right]^2$, hence $\boldsymbol{v} \in \left[H^1_{loc}(\Omega)\right]^2$. We use a result due to Evans and Gariepy (see [63, Section 4.9.2, Theorem 2]), according to which functions in $H^1_{loc}(\Omega)$ are continuous across interior edges in Ω. Thus $[\boldsymbol{v}]|_{e\in\mathcal{E}_{\Omega,h}} = \boldsymbol{0}$. Next, $\boldsymbol{v}_h \in \left[\mathcal{C}(\overline{\Omega})\right]^2$, hence $[\boldsymbol{v}_h] = 0$. Therefore we have $\boldsymbol{v}-\boldsymbol{v}_h|_\Gamma = 0$, and $[\boldsymbol{v}-\boldsymbol{v}_h]|_{e\in\mathcal{E}_{\Omega,h}} = 0$. So

$$\sum_{e\in\mathcal{E}_h}\int_e \{\boldsymbol{T}_h^n\}\boldsymbol{n}_e\cdot[\boldsymbol{v}-\boldsymbol{v}_h] d\sigma = \sum_{e\in\mathcal{E}_{S,h}}\int_e \left(\boldsymbol{T}_h^n\boldsymbol{n}_e\right)_{\boldsymbol{\tau}}\cdot(\boldsymbol{v}_{\boldsymbol{\tau}}-\boldsymbol{v}_{\boldsymbol{\tau}h}) d\sigma.$$

Thus (3.4) is reduced to

$$\begin{cases} a(\boldsymbol{u}-\boldsymbol{u}_h^n,\boldsymbol{v})+b(\boldsymbol{v},p-p_h^n)=\displaystyle\int_\Omega(\boldsymbol{f}-\boldsymbol{f}_K)\cdot(\boldsymbol{v}-\boldsymbol{v}_h)dx \\ \quad+\displaystyle\sum_{K\in\mathcal{T}_h}\int_K(div\,\boldsymbol{T}_h^n+\boldsymbol{f}_K)\cdot(\boldsymbol{v}-\boldsymbol{v}_h)dx \\ \quad-\displaystyle\sum_{e\in\mathcal{E}_{\Omega,h}}\int_e[\boldsymbol{T}_h^n]\boldsymbol{n}_e\cdot(\boldsymbol{v}-\boldsymbol{v}_h)d\sigma-\sum_{e\in\mathcal{E}_{S,h}}\int_e\left[\left(\boldsymbol{T}_h^n\boldsymbol{n}_e\right)_{\boldsymbol{\tau}}+g_e\boldsymbol{\alpha}_h^n\right]\cdot(\boldsymbol{v}_{\boldsymbol{\tau}}-\boldsymbol{v}_{\boldsymbol{\tau}h})d\sigma \\ \quad-\displaystyle\sum_{e\in\mathcal{E}_{S,h}}\int_e g_e(\boldsymbol{\alpha}_h^n-\boldsymbol{\alpha}_h^{n-1})\cdot(\boldsymbol{v}_{\boldsymbol{\tau}h}-\boldsymbol{v}_{\boldsymbol{\tau}})d\sigma+\sum_{e\in\mathcal{E}_{S,h}}\int_e(g-g_e)\boldsymbol{\alpha}_h^{n-1}\cdot(\boldsymbol{v}_{\boldsymbol{\tau}h}-\boldsymbol{v}_{\boldsymbol{\tau}})d\sigma \\ \quad+\displaystyle\sum_{e\in\mathcal{E}_{S,h}}\int_e g(\boldsymbol{\alpha}_h^{n-1}-\boldsymbol{\alpha})\cdot\boldsymbol{v}_{\boldsymbol{\tau}}d\sigma\ . \\ b(\boldsymbol{u}-\boldsymbol{u}_h^n,q)=-b(\boldsymbol{u}_h^n,q)\ , \end{cases} \tag{3.5}$$

and we also have the relation

$$\boldsymbol{\alpha}-\boldsymbol{\alpha}_h^n=P_\Lambda\left(\boldsymbol{\alpha}+\rho g\boldsymbol{u}_{\boldsymbol{\tau}}\right)-P_\Lambda\left(\boldsymbol{\alpha}_h^{n-1}+\rho g\boldsymbol{u}_{\boldsymbol{\tau}h}^n\right)\ . \tag{3.6}$$

For each element $K\in\mathcal{T}_h$, we set $R_1(\boldsymbol{u}_h^n,p_h^n)=\mathrm{div}\boldsymbol{T}_h^n+\boldsymbol{f}_K$ which is the element wise residual accounting for the violation of the momentum balance Eq. (1.1).

$R_2(\boldsymbol{u}_h^n)=\mathrm{div}\boldsymbol{u}_h^n$ is the elementwise residual of $\boldsymbol{u}_h^n$ corresponding to the violation of the incompressibility condition (1.2).

For $e\in\mathcal{E}_{\Omega,h}$, $R_3(\boldsymbol{u}_h^n,p_h^n)=[\boldsymbol{T}_h^n]\boldsymbol{n}_e$ is the inter element jump of the trace operator that associates the weak formulation to the strong formulation.

Finally, for $e\in\mathcal{E}_{S,h}$, $R_4(\boldsymbol{u}_h^n,p_h^n,\boldsymbol{\alpha}_h^n)=(\boldsymbol{T}\boldsymbol{n}_e)_{\boldsymbol{\tau}}+g_e\boldsymbol{\alpha}_h^n$ is an edge residual which account for the slip/stick boundary condition (1.5).

The residual equations (3.5) allows us to deduce the following local estimators in each $K\in\mathcal{T}_h$ and $e\subset K$, and for each iteration n:

1. The estimator stemming in the discretisation is given as follows; for all $K\in\mathcal{T}_h$

$$\begin{aligned}(\eta_{K,D}^n)^2=h_K^2\,||\div\boldsymbol{T}_h^n+\boldsymbol{f}_K||_K^2+||\div\boldsymbol{u}_h^n||_K^2+\sum_{e\in\partial K,\ e\cap\partial\Omega=\emptyset}h_e\,||[\boldsymbol{T}_h^n\boldsymbol{n}_e]||_e^2 \\ +\sum_{e\subset\partial K\cap S}h_e\,||(\boldsymbol{T}_h^n\boldsymbol{n}_e)_{\boldsymbol{\tau}}+g_e\boldsymbol{\alpha}_h^n||_e^2\ .\end{aligned} \tag{3.7}$$

2. The estimator related to the linearization is defined as follows; for any $e\in\mathcal{E}_{S,h}$,

$$(\eta_{e,L}^n)^2=h_e^{1/2}\|\boldsymbol{\alpha}_h^n-\boldsymbol{\alpha}_h^{n-1}\|_e. \tag{3.8}$$

We define the global indicators:

$$(\eta_D^n)^2=\sum_{K\in\mathcal{T}_h}(\eta_{K,D}^n)^2,\quad(\eta_L^n)^2=\sum_{e\in\mathcal{E}_{S,h}}(\eta_{e,L}^n)^2,\ \text{ and }\ (\eta_h^n)^2=(\eta_D^n)^2+(\eta_L^n)^2.$$

Next, we establish the reliability of the error estimator η_h^n.

3.2 Reliability estimates

The goal of this paragraph is to prove the reliability of the *a posteriori* error estimator η_h. The proof is done in several steps, and we derive below an estimate for the velocity error.

Lemma 3.1 *Let* $(\boldsymbol{u}, p, \boldsymbol{\alpha})$ *and* $(\boldsymbol{u}_h^n, p_h^n, \boldsymbol{\alpha}_h^n)$ *be the solutions of* (1.14) *and* (2.9)*, respectively. Assume that* (2.10) *is valid. It holds that*

$$\begin{aligned}\rho\Big(2\nu - \rho c\|g\|^2_{L^\infty(S)}\Big)\|\boldsymbol{u} - \boldsymbol{u}_h^n\|_1^2 \le 4\sum_{e\in\mathcal{E}_{S,h}} h_e^{1/2}\|\boldsymbol{\alpha}_h^{n-1} - \boldsymbol{\alpha}_h^n\|_e \\ + 2\rho\Big(\sum_{K\in\mathcal{T}_h} ||div\,\boldsymbol{u}_h^n||_K^2\Big)^{1/2}||p - p_h^n|| \\ + 2\rho L(\boldsymbol{u} - \boldsymbol{u}_h^n, \boldsymbol{v}_h).\end{aligned}$$

Proof We set

$$\begin{aligned}L(\boldsymbol{v}, \boldsymbol{v}_h) = \int_\Omega (\boldsymbol{f} - \boldsymbol{f}_K)\cdot(\boldsymbol{v} - \boldsymbol{v}_h)dx + \sum_{K\in\mathcal{T}_h}\int_K (div\,\boldsymbol{T}_h^n + \boldsymbol{f}_K)\cdot(\boldsymbol{v} - \boldsymbol{v}_h)dx \\ - \sum_{e\in\mathcal{E}_{\Omega,h}}\int_e [\boldsymbol{T}_h^n]\boldsymbol{n}_e\cdot(\boldsymbol{v} - \boldsymbol{v}_h)d\sigma - \sum_{e\in\mathcal{E}_{S,h}}\int_e \Big[\Big(\boldsymbol{T}_h^n\boldsymbol{n}_e\Big)_{\boldsymbol{\tau}} + g_e\boldsymbol{\alpha}_h^n\Big] \\ \cdot(\boldsymbol{v}_{\boldsymbol{\tau}} - \boldsymbol{v}_{\boldsymbol{\tau}h})d\sigma \\ - \sum_{e\in\mathcal{E}_{S,h}}\int_e g_e(\boldsymbol{\alpha}_h^n - \boldsymbol{\alpha}_h^{n-1})\cdot(\boldsymbol{v}_{\boldsymbol{\tau}h} - \boldsymbol{v}_{\boldsymbol{\tau}})d\sigma \\ + \sum_{e\in\mathcal{E}_{S,h}}\int_e (g - g_e)\boldsymbol{\alpha}_h^{n-1}\cdot(\boldsymbol{v}_{\boldsymbol{\tau}h} - \boldsymbol{v}_{\boldsymbol{\tau}})d\sigma.\end{aligned} \tag{3.9}$$

With (3.9), (3.5) reads

$$a(\boldsymbol{u} - \boldsymbol{u}_h^n, \boldsymbol{v}) + b(\boldsymbol{v}, p - p_h^n) = L(\boldsymbol{v}, \boldsymbol{v}_h) + \sum_{e\in\mathcal{E}_{S,h}}\int_e (\boldsymbol{\alpha}_h^{n-1} - \boldsymbol{\alpha})\cdot(g\boldsymbol{v}_{\boldsymbol{\tau}})d\sigma. \tag{3.10}$$

For $e \in \mathcal{E}_{S,h}$, we take the $L^2(e)$ norm on both sides of (3.6) which together with Lemma 1.2 gives

$$\begin{aligned}\sum_{e\in\mathcal{E}_{S,h}} ||\boldsymbol{\alpha} - \boldsymbol{\alpha}_h^n||_e^2 \le \sum_{e\in\mathcal{E}_{S,h}} ||\boldsymbol{\alpha} - \boldsymbol{\alpha}_h^{n-1}||_e^2 - 2\rho\sum_{e\in\mathcal{E}_{S,h}}((\boldsymbol{\alpha}_h^{n-1} - \boldsymbol{\alpha}), g(\boldsymbol{u}_{\boldsymbol{\tau}} - \boldsymbol{u}_{\boldsymbol{\tau}h}^n))_e \\ + \rho^2||g||^2_{L^\infty(S)}||\boldsymbol{u}_{\boldsymbol{\tau}} - \boldsymbol{u}_{\boldsymbol{\tau}h}^n||_S^2.\end{aligned} \tag{3.11}$$

We take $\boldsymbol{v} = \boldsymbol{u} - \boldsymbol{u}_h^n$ in (3.10), replace the resulting equation in (3.11) and obtain

$$\begin{aligned}\sum_{e\in\mathcal{E}_{S,h}} ||\boldsymbol{\alpha} - \boldsymbol{\alpha}_h^n||_e^2 \leq & \sum_{e\in\mathcal{E}_{S,h}} ||\boldsymbol{\alpha} - \boldsymbol{\alpha}_h^{n-1}||_e^2 \\ & -2\rho\Big(a(\boldsymbol{u} - \boldsymbol{u}_h^n, \boldsymbol{u} - \boldsymbol{u}_h^n) + b(\boldsymbol{u} - \boldsymbol{u}_h^n, p - p_h^n) - L(\boldsymbol{u} - \boldsymbol{u}_h^n, \boldsymbol{v}_h)\Big) \\ & +\rho^2 ||g||_{L^\infty(S)}^2 ||\boldsymbol{u}_{\boldsymbol{\tau}} - \boldsymbol{u}_{\boldsymbol{\tau},h}^n||_S^2,\end{aligned}$$

which from the coercivity of $a(\cdot,\cdot)$ (using (2.2)) and trace's inequality lead to

$$\begin{aligned}&\rho\Big(2\nu - \rho c\|g\|_{L^\infty(S)}^2\Big)\|\boldsymbol{u} - \boldsymbol{u}_h^n\|_1^2 \\ &\leq \sum_{e\in\mathcal{E}_{S,h}} \|\boldsymbol{\alpha} - \boldsymbol{\alpha}_h^{n-1}\|_e^2 - \sum_{e\in\mathcal{E}_{S,h}} ||\boldsymbol{\alpha} - \boldsymbol{\alpha}_h^n||_e^2 + 2\rho L(\boldsymbol{u} - \boldsymbol{u}_h^n, \boldsymbol{v}_h) - 2\rho b(\boldsymbol{u} - \boldsymbol{u}_h^n, p - p_h^n) \\ &= \sum_{e\in\mathcal{E}_{S,h}} \Big(||\boldsymbol{\alpha} - \boldsymbol{\alpha}_h^{n-1}||_e - ||\boldsymbol{\alpha} - \boldsymbol{\alpha}_h^n||_e\Big)\Big(||\boldsymbol{\alpha} - \boldsymbol{\alpha}_h^{n-1}||_e + ||\boldsymbol{\alpha} - \boldsymbol{\alpha}_h^n||_e\Big) \\ &\quad + 2\rho L(\boldsymbol{u} - \boldsymbol{u}_h^n, \boldsymbol{v}_h) - 2\rho b(\boldsymbol{u} - \boldsymbol{u}_h^n, p - p_h^n) \\ &\leq \sum_{e\in\mathcal{E}_{S,h}} ||\boldsymbol{\alpha}_h^{n-1} - \boldsymbol{\alpha}_h^n||_e \Big(2||\boldsymbol{\alpha}||_e + ||\boldsymbol{\alpha}_h^{n-1}||_e + ||\boldsymbol{\alpha}_h^n||_e\Big) \\ &\quad + 2\rho L(\boldsymbol{u} - \boldsymbol{u}_h^n, \boldsymbol{v}_h) - 2\rho b(\boldsymbol{u} - \boldsymbol{u}_h^n, p - p_h^n) \\ &\leq 4\sum_{e\in\mathcal{E}_{S,h}} h_e^{1/2}\|\boldsymbol{\alpha}_h^{n-1} - \boldsymbol{\alpha}_h^n\|_e + 2\rho L(\boldsymbol{u} - \boldsymbol{u}_h^n, \boldsymbol{v}_h) - 2\rho b(\boldsymbol{u} - \boldsymbol{u}_h^n, p - p_h^n).\end{aligned} \tag{3.12}$$

In the last inequality of (3.12), one notes that because $|\boldsymbol{\alpha}| \leq 1$ and $|\boldsymbol{\alpha}_h^n| \leq 1$, we have $||\boldsymbol{\alpha}||_e^2 \leq h_e$, and $||\boldsymbol{\alpha}_h^n||_e^2 \leq h_e$. It remains to estimate $b(\boldsymbol{u} - \boldsymbol{u}_h^n, p_h^n - p)$. For that purpose, we quickly see that

$$\begin{aligned}b(\boldsymbol{u} - \boldsymbol{u}_h^n, p_h^n - p) = & \underbrace{b(\boldsymbol{u}, p_h^n - p)}_{=0} - b(\boldsymbol{u}_h^n, p_h^n - p) \\ & \leq \sum_{K\in\mathcal{T}_h} \|div\, \boldsymbol{u}_h^n\|_K \|p - p_h^n\|_K \\ & \leq \Big(\sum_{K\in\mathcal{T}_h} ||div\, \boldsymbol{u}_h^n||_K^2\Big)^{1/2} ||p - p_h^n||.\end{aligned} \tag{3.13}$$

Returning to (3.12) with (3.13), we get the desired estimate. □

In the light of Lemma 3.1, we need to estimate $L(\boldsymbol{u} - \boldsymbol{u}_h^n, \boldsymbol{v}_h)$ for particular $\boldsymbol{v}_h$ and $\|p - p_h^n\|$. Having the expression of $L(\boldsymbol{v}, \boldsymbol{v}_h)$ given in (3.9), we can write

$$L(\boldsymbol{u} - \boldsymbol{u}_h^n, \boldsymbol{v}_h) = T_1 + T_2 + T_3 + T_4 + T_5, \tag{3.14}$$

with

$$
\begin{aligned}
T_1 &= \sum_{K\in\mathcal{T}_h}\int_K (div\,\boldsymbol{T}_h^n + \boldsymbol{f}_K)\cdot(\boldsymbol{u}-\boldsymbol{u}_h^n-\boldsymbol{v}_h)dx \\
&\quad + \sum_{K\in\mathcal{T}_h}\int_K (\boldsymbol{f}-\boldsymbol{f}_K)\cdot(\boldsymbol{u}-\boldsymbol{u}_h^n-\boldsymbol{v}_h)dx \\
T_2 &= -\sum_{e\in\mathcal{E}_{\Omega,h}}\int_e [\boldsymbol{T}_h^n]\boldsymbol{n}_e\cdot\{\boldsymbol{u}-\boldsymbol{u}_h^n-\boldsymbol{v}_h\}\,d\sigma \\
T_3 &= -\sum_{e\in\mathcal{E}_{S,h}}\int_e (g-g_e)\boldsymbol{\alpha}_h^{n-1}\cdot(\boldsymbol{u}_{\boldsymbol{\tau}}-\boldsymbol{u}_{\boldsymbol{\tau}h}^n-\boldsymbol{v}_{\boldsymbol{\tau}h})d\sigma \\
T_4 &= -\sum_{e\in\mathcal{E}_{S,h}}\int_e ((\boldsymbol{T}_h^n\boldsymbol{n}_e)_{\boldsymbol{\tau}}+g_e\boldsymbol{\alpha}_h^n)\cdot(\boldsymbol{u}_{\boldsymbol{\tau}}-\boldsymbol{u}_{\boldsymbol{\tau}h}^n-\boldsymbol{v}_{\boldsymbol{\tau}h})d\sigma \\
T_5 &= \sum_{e\in\mathcal{E}_{S,h}}\int_e g_e(\boldsymbol{\alpha}_h^n-\boldsymbol{\alpha}_h^{n-1})\cdot(\boldsymbol{u}_{\boldsymbol{\tau}}-\boldsymbol{u}_{\boldsymbol{\tau}h}^n-\boldsymbol{v}_{\boldsymbol{\tau}h})d\sigma.
\end{aligned}
$$

Using standard inequalities, we derive below an estimate of $L(\boldsymbol{u}-\boldsymbol{u}_h^n,\boldsymbol{v}_h)$ for $\boldsymbol{v}_h=\mathcal{R}_h(\boldsymbol{u}-\boldsymbol{u}_h^n)$.

Lemma 3.2 *It holds that*

$$
\begin{aligned}
L(\boldsymbol{u}-\boldsymbol{u}_h^n,\mathcal{R}_h(\boldsymbol{u}-\boldsymbol{u}_h^n)) &\le c\Bigg[\Big(\sum_{K\in\mathcal{T}_h}h_K^2||div\,\boldsymbol{T}_h^n+\boldsymbol{f}_K||_K^2\Big)^{1/2}+\Big(\sum_{e\in\mathcal{E}_{\Omega,h}}h_e||[\boldsymbol{T}_h^n]||_e^2\Big)^{1/2} \\
&+\Big(\sum_{e\in\mathcal{E}_{S,h}}h_e||(\boldsymbol{T}_h^n\boldsymbol{n}_e)_{\boldsymbol{\tau}}+g_e\boldsymbol{\alpha}_h^n||_e^2\Big)^{1/2}+\|g\|_{L^\infty(S)}\Big(\sum_{e\in\mathcal{E}_{S,h}}h_e||\boldsymbol{\alpha}_h^n-\boldsymbol{\alpha}_h^{n-1}||_e^2\Big)^{1/2} \\
&+\Big(\sum_{e\in\mathcal{E}_{S,h}}h_e||g-g_e||_e^2\Big)^{1/2}\Bigg]\|\boldsymbol{u}-\boldsymbol{u}_h^n\|_1.
\end{aligned}
$$

Proof T_1 is bounded by using the inequalities of Cauchy–Schwarz, Hölder and (3.2) as follows

$$
\begin{aligned}
T_1 &= \sum_{K\in\mathcal{T}_h}\int_K (div\,\boldsymbol{T}_h^n+\boldsymbol{f}_K)\cdot(\boldsymbol{u}-\boldsymbol{u}_h^n-\mathcal{R}_h(\boldsymbol{u}-\boldsymbol{u}_h^n))dx \\
&\quad+\sum_{K\in\mathcal{T}_h}\int_K(\boldsymbol{f}-\boldsymbol{f}_K)\cdot(\boldsymbol{u}-\boldsymbol{u}_h^n-\mathcal{R}_h(\boldsymbol{u}-\boldsymbol{u}_h^n))dx \\
&\le\Big(\sum_{K\in\mathcal{T}_h}h_K^2||div\,\boldsymbol{T}_h^n+\boldsymbol{f}_K||_K^2\Big)^{1/2}\Big(\sum_{K\in\mathcal{T}_h}h_K^{-2}||\boldsymbol{u}-\boldsymbol{u}_h^n-\mathcal{R}_h(\boldsymbol{u}-\boldsymbol{u}_h^n)||_K^2\Big)^{1/2}
\end{aligned}
$$

$$
\begin{aligned}
&+\Big(\sum_{K\in\mathcal{T}_h} h_K^2||\boldsymbol{f}-\boldsymbol{f}_K||_K^2\Big)^{1/2}\Big(\sum_{K\in\mathcal{T}_h} h_K^{-2}||\boldsymbol{u}-\boldsymbol{u}_h^n-\mathcal{R}_h(\boldsymbol{u}-\boldsymbol{u}_h^n)||_K^2\Big)^{1/2}\\
&\le c\Big(\sum_{K\in\mathcal{T}_h} h_K^2||div\,\boldsymbol{T}_h^n+\boldsymbol{f}_K||_K^2\Big)^{1/2}||\boldsymbol{u}-\boldsymbol{u}_h^n||_1\\
&\quad+\Big(\sum_{K\in\mathcal{T}_h} h_K^2||\boldsymbol{f}-\boldsymbol{f}_K||_K^2\Big)^{1/2}||\boldsymbol{u}-\boldsymbol{u}_h^n||_1.
\end{aligned}
$$

Next, we introduce the discrete trace inequality [64, Section 1.6]:

$$
\begin{aligned}
&\text{For all } p\in[1,\infty],\ \text{ all } (v,K)\in W^{1,p}(K)\times\mathcal{T}_h \text{ and all faces } e\subset K,\\
&\qquad \|v\|_{L^p(e)}\le c\Big(h_K^{-1/p}\|\boldsymbol{v}\|_{L^p(K)}+h_K^{1-1/p}\|\nabla\boldsymbol{v}\|_{L^p(K)}\Big),
\end{aligned}
\tag{3.15}
$$

where c is a constant independent of h. Now, T_2 is treated with Cauchy–Schwarz's, Hölder's inequalities, (3.15) and (3.2) as follows

$$
\begin{aligned}
T_2 &= -\sum_{e\in\mathcal{E}_{\Omega,h}}\int_e [\boldsymbol{T}_h^n]\boldsymbol{n}_e\cdot\{\boldsymbol{u}-\boldsymbol{u}_h^n-\mathcal{R}_h(\boldsymbol{u}-\boldsymbol{u}_h^n)\}\,d\sigma\\
&\le \Big(\sum_{e\in\mathcal{E}_{\Omega,h}} h_e||[\boldsymbol{T}_h^n]||_e^2\Big)^{1/2}\Big(\sum_{e\in\mathcal{E}_{\Omega,h}} h_e^{-1}||\{\boldsymbol{u}-\boldsymbol{u}_h^n-\mathcal{R}_h(\boldsymbol{u}-\boldsymbol{u}_h^n)\}||_e^2\Big)^{1/2}\\
&\le c\Big(\sum_{e\in\mathcal{E}_{\Omega,h}} h_e||[\boldsymbol{T}_h^n]||_e^2\Big)^{1/2}\Big(\sum_{K\in\mathcal{T}_h} h_K^{-2}||\boldsymbol{u}-\boldsymbol{u}_h^n-\mathcal{R}_h(\boldsymbol{u}-\boldsymbol{u}_h^n)||_K^2\\
&\qquad+||\nabla(\boldsymbol{u}-\boldsymbol{u}_h^n-\mathcal{R}_h(\boldsymbol{u}-\boldsymbol{u}_h^n))||_K\Big)^{1/2}\\
&\le c\Big(\sum_{e\in\mathcal{E}_{\Omega,h}} h_e||[\boldsymbol{T}_h^n]||_e^2\Big)^{1/2}||\boldsymbol{u}-\boldsymbol{u}_h^n||_1.
\end{aligned}
$$

Using the same arguments as the bound of T_2 with $|\boldsymbol{\alpha}_h^{n-1}|\le 1$, we have

$$
\begin{aligned}
T_3 &= -\sum_{e\in\mathcal{E}_{S,h}}\int_e (g-g_e)\boldsymbol{\alpha}_h^{n-1}\cdot(\boldsymbol{u}_{\boldsymbol{\tau}}-\boldsymbol{u}_{\boldsymbol{\tau}h}^n-\mathcal{R}_h(\boldsymbol{u}_{\boldsymbol{\tau}}-\boldsymbol{u}_{\boldsymbol{\tau}h}^n))d\sigma\\
&\le \Big(\sum_{e\in\mathcal{E}_{S,h}} h_e||g-g_e||_e^2\Big)^{1/2}\Big(\sum_{e\in\mathcal{E}_{S,h}} h_e^{-1}||\boldsymbol{u}_{\boldsymbol{\tau}}-\boldsymbol{u}_{\boldsymbol{\tau}h}^n-\mathcal{R}_h(\boldsymbol{u}_{\boldsymbol{\tau}}-\boldsymbol{u}_{\boldsymbol{\tau}h}^n)||_e^2\Big)^{1/2}\\
&\le c\Big(\sum_{e\in\mathcal{E}_{S,h}} h_e||g-g_e||_e^2\Big)^{1/2}||\boldsymbol{u}-\boldsymbol{u}_h^n||_1,
\end{aligned}
$$

and

$$T_4 \le c\Big(\sum_{e\in\mathcal{E}_{S,h}} h_e||(\boldsymbol{T}_h^n\boldsymbol{n}_e)_{\boldsymbol{\tau}} + g_e\boldsymbol{\alpha}_h^n||_e^2\Big)^{1/2}||\boldsymbol{u}-\boldsymbol{u}_h^n||_1$$

$$T_5 \le c\Big(\sum_{e\in\mathcal{E}_{S,h}} h_e||g_e(\boldsymbol{\alpha}_h^n-\boldsymbol{\alpha}_h^{n-1})||_e^2\Big)^{1/2}||\boldsymbol{u}-\boldsymbol{u}_h^n||_1$$

$$\le c\|g\|_{L^\infty(S)}\Big(\sum_{e\in\mathcal{E}_{S,h}} h_e||\boldsymbol{\alpha}_h^n-\boldsymbol{\alpha}_h^{n-1}||_e^2\Big)^{1/2}||\boldsymbol{u}-\boldsymbol{u}_h^n||_1.$$

We return to (3.14) with the estimates for T_i and obtain the desired estimate. □

From Lemmas 3.1 and 3.2, we obtain

$$\rho\Big(2\nu-\rho c\|g\|_{L^\infty(S)}^2\Big)\|\boldsymbol{u}-\boldsymbol{u}_h^n\|_1^2 \le 4\sum_{e\in\mathcal{E}_{S,h}} h_e^{1/2}\|\boldsymbol{\alpha}_h^{n-1}-\boldsymbol{\alpha}_h^n\|_e$$
$$+2\rho\Big(\sum_{K\in\mathcal{T}_h}||div\,\boldsymbol{u}_h^n||_K^2\Big)^{1/2}||p-p_h^n||$$
$$+\rho c\Big[\Big(\sum_{K\in\mathcal{T}_h} h_K^2||div\,\boldsymbol{T}_h^n+\boldsymbol{f}_K||_K^2\Big)^{1/2}+\Big(\sum_{e\in\mathcal{E}_{\Omega,h}} h_e||[\boldsymbol{T}_h^n]||_e^2\Big)^{1/2}$$
$$+\Big(\sum_{e\in\mathcal{E}_{S,h}} h_e||(\boldsymbol{T}_h^n\boldsymbol{n}_e)_{\boldsymbol{\tau}}+g_e\boldsymbol{\alpha}_h^n||_e^2\Big)^{1/2}+\|g\|_{L^\infty(S)}\Big(\sum_{e\in\mathcal{E}_{S,h}} h_e||\boldsymbol{\alpha}_h^n-\boldsymbol{\alpha}_h^{n-1}||_e^2\Big)^{1/2}$$
$$+\Big(\sum_{e\in\mathcal{E}_{S,h}} h_e||g-g_e||_e^2\Big)^{1/2}\Big]\|\boldsymbol{u}-\boldsymbol{u}_h^n\|_1 \tag{3.16}$$

We apply the inequality of Young ($ab \le \frac{\varepsilon}{2}a^2+\frac{1}{2\varepsilon}b^2$ with $a=\|\boldsymbol{u}-\boldsymbol{u}_h^n\|_1$ and $\varepsilon=\rho(2\nu-\rho c\|g\|_{L^\infty(S)}^2)$) on the right hand side of (3.16) and using (2.10), to get

$$\|\boldsymbol{u}-\boldsymbol{u}_h^n\|_1^2 \le c_1\sum_{e\in\mathcal{E}_{S,h}} h_e^{1/2}\|\boldsymbol{\alpha}_h^{n-1}-\boldsymbol{\alpha}_h^n\|_e+c_2\Big(\sum_{K\in\mathcal{T}_h}||div\,\boldsymbol{u}_h^n||_K^2\Big)^{1/2}||p-p_h^n||$$
$$+c_3\Big(\sum_{K\in\mathcal{T}_h} h_K^2||div\,\boldsymbol{T}_h^n+\boldsymbol{f}_K||_K^2+\sum_{e\in\mathcal{E}_{\Omega,h}} h_e||[\boldsymbol{T}_h^n]||_e^2$$
$$+\sum_{e\in\mathcal{E}_{S,h}} h_e||(\boldsymbol{T}_h^n\boldsymbol{n}_e)_{\boldsymbol{\tau}}+g_e\boldsymbol{\alpha}_h^n||_e^2+\sum_{e\in\mathcal{E}_{S,h}} h_e||\boldsymbol{\alpha}_h^n-\boldsymbol{\alpha}_h^{n-1}||_e^2$$
$$+\sum_{e\in\mathcal{E}_{S,h}} h_e||g-g_e||_e^2+\sum_{K\in\mathcal{T}_h} h_K^2||\boldsymbol{f}-\boldsymbol{f}_K||_K^2\Big), \tag{3.17}$$

where c_1, c_2, c_3 are positive constant independent of h_K but depending on ν, g.

It is manifest that to close the inequality (3.17), we need to estimate $\|p_h^n - p\|$. We have the following result

Lemma 3.3 *It holds that*

$$||p - p_h^n|| \leq c\Bigg[\Bigg(\sum_{K\in\mathcal{T}_h} h_K^2 ||\boldsymbol{f} - \boldsymbol{f}_K||_K^2\Bigg)^{1/2} + \Bigg(\sum_{K\in\mathcal{T}_h} h_K^2 ||div\, \boldsymbol{T}_h^n + \boldsymbol{f}_K||_K^2\Bigg)^{1/2} + \Bigg(\sum_{e\in\mathcal{E}_{\Omega,h}} h_e ||[\boldsymbol{T}_h^n]||_e^2\Bigg)^{1/2} + 2\nu||\boldsymbol{u} - \boldsymbol{u}_h^n||_1\Bigg].$$

The proof is inspired from similar result in [39, Lemma 1].

Proof The pair $(\mathbb{V}\cap\{\boldsymbol{v}|_S = 0\}, M)$ is inf-sup stable. Hence there exists $\boldsymbol{w} \in \mathbb{V}\cap\{\boldsymbol{v}|_S = 0\}$ such that

$$\|p - p_h^n\|^2 = b(\boldsymbol{w}, p - p_h^n) \quad \text{and} \quad \|\boldsymbol{w}\|_1 \leq c\|p - p_h^n\|. \tag{3.18}$$

Let $\boldsymbol{w}^I \in \mathbb{V}_h \cap \{\boldsymbol{v}|_S = 0\}$, the an interpolant of $\boldsymbol{w}$ ($\boldsymbol{w}^I$ is an operator of Clément (see [64])) such that

$$|\boldsymbol{w} - \boldsymbol{w}^I|_{s,K} \leq c h_K^{1-s} |\boldsymbol{w}|_{1,K}\,, \quad \text{for all } K \in \mathcal{T}_h,\ 0 \leq s \leq 1. \tag{3.19}$$

The difference between (1.10) and (2.9) gives

$$a(\boldsymbol{u}_h^n - \boldsymbol{u}, \boldsymbol{v}) + b(\boldsymbol{v}, p_h^n - p) = 0 \ \text{ for all } \ \boldsymbol{v} \in \mathbb{V}_h \cap \{\boldsymbol{v}|_S = 0\}. \tag{3.20}$$

For $\boldsymbol{v} = \boldsymbol{w}^I$ in (3.20), it holds that

$$\begin{aligned} b(\boldsymbol{w}, p - p_h^n) &= b(\boldsymbol{w} - \boldsymbol{w}^I, p - p_h^n) + b(\boldsymbol{w}^I, p - p_h^n) \\ &= b(\boldsymbol{w} - \boldsymbol{w}^I, p - p_h^n) + a(\boldsymbol{u} - \boldsymbol{u}_h^n, \boldsymbol{w}^I) \\ &= b(\boldsymbol{w} - \boldsymbol{w}^I, p - p_h^n) + a(\boldsymbol{u} - \boldsymbol{u}_h^n, \boldsymbol{w}^I - \boldsymbol{w}) + a(\boldsymbol{u} - \boldsymbol{u}_h^n, \boldsymbol{w}) \\ &= (\boldsymbol{f}, \boldsymbol{w} - \boldsymbol{w}^I) - b(\boldsymbol{w} - \boldsymbol{w}^I, p_h^n) - a(\boldsymbol{u}_h^n, \boldsymbol{w}^I - \boldsymbol{w}) + a(\boldsymbol{u} - \boldsymbol{u}_h^n, \boldsymbol{w}), \end{aligned} \tag{3.21}$$

where we have used the fact that $(\boldsymbol{u}, p)$ is the continuous solution with $\boldsymbol{w} - \boldsymbol{w}^I \in \mathbb{V}\cap\{\boldsymbol{v}|_S = \boldsymbol{0}\}$.

From (3.1), and $\boldsymbol{w} - \boldsymbol{w}^I|_{\partial\Omega} = \boldsymbol{0}$, we have

$$-b(\boldsymbol{w} - \boldsymbol{w}^I, p_h^n) - a(\boldsymbol{u}_h^n, \boldsymbol{w}^I - \boldsymbol{w}) = \sum_{K\in\mathcal{T}_h}\int_K \div \boldsymbol{T}_h^n \cdot (\boldsymbol{w}^I - \boldsymbol{w})dx - \sum_{e\in\mathcal{E}_{\Omega,h}}\int_e [\boldsymbol{T}_h^n]\boldsymbol{n}_e \cdot \{\boldsymbol{w}^I - \boldsymbol{w}\}d\sigma.$$

Thus (3.21) becomes

$$\begin{aligned} b(\boldsymbol{w}, p-p_h^n) &= \sum_{K\in\mathcal{T}_h}\int_K \boldsymbol{f}\cdot(\boldsymbol{w}-\boldsymbol{w}^I)dx + \sum_{K\in\mathcal{T}_h}\int_K div\boldsymbol{T}_h^n\cdot(\boldsymbol{w}^I-\boldsymbol{w})dx \\ &\quad - \sum_{e\in\mathcal{E}_{\Omega,h}}\int_e [\boldsymbol{T}_h^n]\boldsymbol{n}_e\cdot\{\boldsymbol{w}^I-\boldsymbol{w}\}d\sigma + a(\boldsymbol{u}-\boldsymbol{u}_h^n,\boldsymbol{w}) \\ &= \sum_{K\in\mathcal{T}_h}\int_K (\boldsymbol{f}-\boldsymbol{f}_K)\cdot(\boldsymbol{w}-\boldsymbol{w}^I)dx \\ &\quad + \sum_{K\in\mathcal{T}_h}\int_K (div\,\boldsymbol{T}_h^n+\boldsymbol{f}_K)\cdot(\boldsymbol{w}^I-\boldsymbol{w})dx \\ &\quad - \sum_{e\in\mathcal{E}_{\Omega,h}}\int_e [\boldsymbol{T}_h^n]\boldsymbol{n}_e\cdot\{\boldsymbol{w}^I-\boldsymbol{w}\}d\sigma + a(\boldsymbol{u}-\boldsymbol{u}_h^n,\boldsymbol{w}). \end{aligned} \tag{3.22}$$

Now, following the estimation of T_i given in (3.14) and using (3.18) and (3.19), (3.22) is bounded as follows

$$\begin{aligned} b(\boldsymbol{w}, p-p_h^n) \le c\Big[\Big(\sum_{K\in\mathcal{T}_h} h_K^2||\boldsymbol{f}-\boldsymbol{f}_K||_K^2\Big)^{1/2}||\boldsymbol{w}||_1 + \Big(\sum_{K\in\mathcal{T}_h} h_K^2||\div\boldsymbol{T}_h^n+\boldsymbol{f}_K||_K^2\Big)^{1/2}||\boldsymbol{w}||_1 \\ + \Big(\sum_{e\in\mathcal{E}_{\Omega,h}} h_e||[\boldsymbol{T}_h^n]||_e^2\Big)^{1/2}||\boldsymbol{w}||_1 + 2\nu||\boldsymbol{u}-\boldsymbol{u}_h^n||_1||\boldsymbol{w}||_1\Big], \end{aligned}$$

which together with (3.18) gives the desired estimate.

Using Lemmas 3.1, 3.2 and 3.3, we state and deduce the main result of this paragraph

Theorem 3.1 *Let* $(\boldsymbol{u}, p, \boldsymbol{\alpha})$ *and* $(\boldsymbol{u}_h^n, p_h^n, \boldsymbol{\alpha}_h^n)$ *be the solutions of* (1.14) *and* (2.9)*, respectively. Assume that* (2.10) *is valid. Then it holds that*

$$\|\boldsymbol{u}-\boldsymbol{u}_h^n\|_1^2 + \|p-p_h^n\|^2 \le c\Big((\eta_h^n)^2 + \sum_{K\in\mathcal{T}_h} h_K^2\,||\,\boldsymbol{f}-\boldsymbol{f}_K\,||_K^2 + \sum_{e\in\mathcal{E}_{S,h}} h_e\,||\,g-g_e\,||_e^2\Big),$$

where c is positive constant independent of h and n.

Proof The estimate obtained in Lemma 3.3 is replaced in (3.17) and after application of the inequality of Young, we obtain

$$\begin{aligned} ||\boldsymbol{u}-\boldsymbol{u}_h^n||_1^2 \le c\Big(&\sum_{K\in\mathcal{T}_h}||div\,\boldsymbol{u}_h^n||_K^2 + \sum_{e\in\mathcal{E}_{S,h}} h_e^{1/2}||\boldsymbol{\alpha}_h^{n-1}-\boldsymbol{\alpha}_h^n||_e \\ &+ \sum_{K\in\mathcal{T}_h} h_K^2||div\,\boldsymbol{T}_h^n+\boldsymbol{f}_K||_K^2 + \sum_{K\in\mathcal{T}_h} h_K^2||\boldsymbol{f}-\boldsymbol{f}_K||_K^2 + \sum_{e\in\mathcal{E}_{\Omega,h}} h_e||[\boldsymbol{T}_h^n]||_e^2 \\ &+ \sum_{e\in\mathcal{E}_{S,h}} h_e||g-g_e||_e^2 + \sum_{e\in\mathcal{E}_{S,h}} h_e||(\boldsymbol{T}_h^n\boldsymbol{n}_e)_{\boldsymbol{\tau}}+g_e\boldsymbol{\alpha}_h^n||_e^2 \end{aligned}$$

$$+ \sum_{e\in\mathcal{E}_{S,h}} h_e ||\boldsymbol{\alpha}_h^n - \boldsymbol{\alpha}_h^{n-1}||_e^2\Big). \tag{3.23}$$

Finally (3.23) and the error estimate on the pressure in Lemma 3.3 ends the proof. □

Remark 3.1 From Theorem 3.1, we note that if $\eta_L^n = 0$ then $\eta_h^n = \eta_D^n$ which is also the estimator obtained in [39].

Remark 3.2 Using the inequality of the triangle, we have

$$(\eta_L^n)^2 \leq h_e^{1/2}\|\boldsymbol{\alpha}_h^n - \boldsymbol{\alpha}\|_e + h_e^{1/2}\|\boldsymbol{\alpha} - \boldsymbol{\alpha}_h^{n-1}\|_e.$$

Thus we need to bound $\|\boldsymbol{\alpha} - \boldsymbol{\alpha}_h^{n-1}\|_e$ in terms of the error on the velocity and the pressure. Using (3.6) and Lemma 1.2, it holds that

$$\sum_{e\in\mathcal{E}_{S,h}} \|\boldsymbol{\alpha} - \boldsymbol{\alpha}_h^n\|_e \leq \sum_{e\in\mathcal{E}_{S,h}} \|\boldsymbol{\alpha} - \boldsymbol{\alpha}_h^{n-1}\|_e + \rho\|g\|_{L^\infty(S)} \sum_{e\in\mathcal{E}_{S,h}} \|\boldsymbol{u}_{\boldsymbol{\tau}} - \boldsymbol{u}_{\boldsymbol{\tau}\,h}^n\|_e\,,$$

which enable to deduce that

$$\sum_{e\in\mathcal{E}_{S,h}} \|\boldsymbol{\alpha} - \boldsymbol{\alpha}_h^n\|_e \leq \sum_{e\in\mathcal{E}_{S,h}} \|\boldsymbol{\alpha} - \boldsymbol{\alpha}_h^0\|_e + \rho\|g\|_{L^\infty(S)} \sum_{i=1}^{n} \sum_{e\in\mathcal{E}_{S,h}} \|\boldsymbol{u} - \boldsymbol{u}_h^i\|_e\,. \tag{3.24}$$

It is manifest from (3.24) that we need (at least) to bound $\|\boldsymbol{\alpha} - \boldsymbol{\alpha}_h^0\|_e$ in terms of the error on the velocity and the pressure, something that we are not capable of doing now. The efficiency of the indicators will be the goal of a future work.

4 Numerical simulations

This section is devoted to the numerical experiments to illustrate the theoretical results discussed in this paper. We use the iterative scheme (2.9) to compute the solution. All the numerical simulations showed in this section are performed with FreeFem code [65]. The starting solution is obtained by taking $\boldsymbol{u}_h^0$ as the solution of (2.9) with $g = 0$. For the stopping criterion given later, we define the relative error as follows

$$Err_L = \frac{\|\boldsymbol{u}_h^{n+1} - \boldsymbol{u}_h^n\|_1 + \|p_h^{n+1} - p_h^n\|}{\|\boldsymbol{u}_h^{n+1}\|_1 + \|p_h^{n+1}\|}.$$

In all examples, $\mathbb{V}_h$ and M_h are given by (2.3) and (2.4).

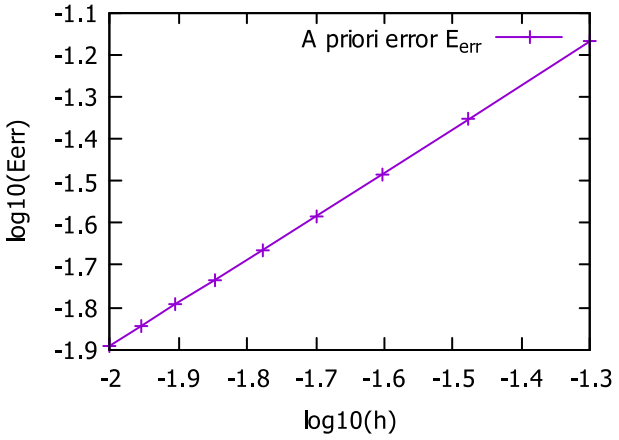


Fig. 1 The a priori error estimate E_{err} with respect to the mesh step h in logarithmic scale

4.1 Example 1

We consider the domain $\Omega = (0, 1)^2$. The uniform mesh is obtained by dividing Ω into N^2 equal squares, each one subdivided into 2 triangles, so that the triangulation consists of $2N^2$ triangles. We set

$$\boldsymbol{f} = (f_1, f_2) \quad \text{where} \quad f_1 = f_2 = 10\, e^{(-100((x-0.8)^2+(y-0.3)^2))},$$

$\nu = 0.5$, $\rho = 0.2$ and $g = 0.2$. We take the Tresca's boundary condition (1.5) on $S = \{(1, y)|\ \text{with}\ \ 0 \leq y \leq 1\}$, and the homogeneous Dirichlet boundary condition $\boldsymbol{u} = \boldsymbol{0}$ on $\partial\Omega\backslash S$.

A priori error estimate. We validate the *a priori error* estimate given in Remark 2.1. Since we do not have the exact solution $(\boldsymbol{u}, p)$ corresponding to this case, we designate the reference solution $(\boldsymbol{u}_{ref}, p_{ref})$, as the numerical solution of (2.9) using Taylor-Hood finite element ($\mathbb{P}_2 \times \mathbb{P}_1$ for the velocity and pressure) for $N = 200$. Next, we compute the numerical solution for $N = 20, 30, 40, \ldots, 100$. Figure 1 shows the graph of the relative error

$$E_{err} = \frac{\|\boldsymbol{u}_{ref} - \boldsymbol{u}_h\|_1 + \|p_{ref} - p_h\|}{\|\boldsymbol{u}_{ref}\|_1 + \|p_{ref}\|}$$

with respect to $h = \dfrac{1}{N}$ in logarithmic scale. The slope of that line is 1.03 which is in agreement with the theoretical result (see Remark 2.1 when $\boldsymbol{u}_{\boldsymbol{\tau}}$ is an element of $\left[H^2(S)\right]^2$).

To show the dependency of $\boldsymbol{u}_{\boldsymbol{\tau},h} = (0, u_{2h})$ with respect to g on $S = \{(1, y)\ |\ \text{with}\ \ 0 \leq y \leq 1\}$, we plot in Fig. 2 the graph of $g \longmapsto u_{2h}$ for $g = 0.05, 0.1, 0.2, 0.3, 0.4, 1$. We note that when g increases, the values of second component of $\boldsymbol{u}_{\boldsymbol{\tau},h}$ decreases.

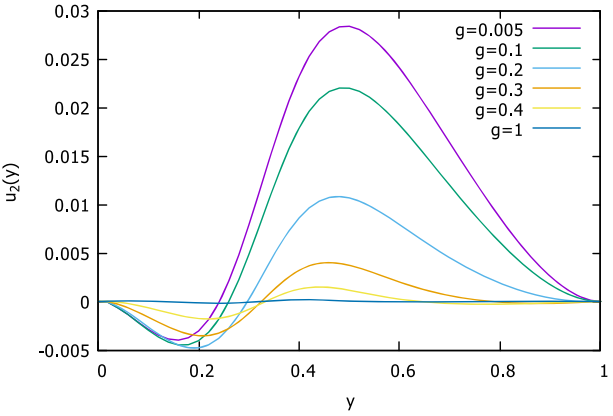


Fig. 2 $\boldsymbol{u}_{\boldsymbol{\tau},h}$ at the line $x = 1$ and $0 \leq y \leq 1$ for $g = 0.05, 0.1, 0.2, 0.3, 0.4, 1$

A posteriori error estimate. In this paragraph, we report on the numerical investigations concerning the a posteriori error estimate. We take $N = 30$ for the uniform initial mesh.

On a given mesh and for the numerical calculation, the iterations are stopped following the criteria

$$\eta_L^n \leq \gamma \eta_D^n, \tag{4.1}$$

where γ is a positive parameter. We note that the stopping condition (4.1) was first formulated and studied in [53, 66] for $\gamma = 0.1$, and used later by many authors (see [49, 50, 54, 55] just to cite a few). In fact, the parameter γ and the stopping criteria (4.1) are very important to avoid unnecessary iterations when the total error is dominated by the discretization one. To illustrate the dependency of the convergence with γ, Fig. 3 shows the evolution of the indicators of discretization $(log_{10}(\eta_D^n))$ and iteration $(log_{10}(\eta_L^n))$ with respect to number of iterations for $g = 0.2, 0.5$ and 1. We present also in the same figures the vertical lines representing the number of iterations when the stopping criteria (4.1) is reached for $\gamma = 0.1$. The criterion (4.1) is reached after 250 iterations for $g = 0.2$, after 63 iterations for $g = 0.5$ and after 20 iterations for $g = 1$.

The adaptive mesh refinement algorithm based on (3.7), and (3.8) can be outlined as follows (see [55]):

We note that the Algorithm 1 uses routines in FreeFem++ based on $\eta_{K,D}^n$ in order to adapt the mesh during the process. The main idea can be summarized as follow: we calculate the mean value η_n^* of the estimators $\eta_{K,D}^n$ at each step n, detect the elements of the mesh where the corresponding estimators are larger then η_i^* and refine them.

In Fig. 4, we present the evolution of the mesh during the iterations (initial, first, second and third refinement level). We notice that more activities are concentrated in some areas. These are (i) the region where the force $\boldsymbol{f}$ is acting, and (ii) the friction zone S (this is the right part of the boundary $\partial\Omega$ corresponding to $x = 1$). Furthermore, Fig. 5 show the velocity during the refinement process corresponding to the above meshes.

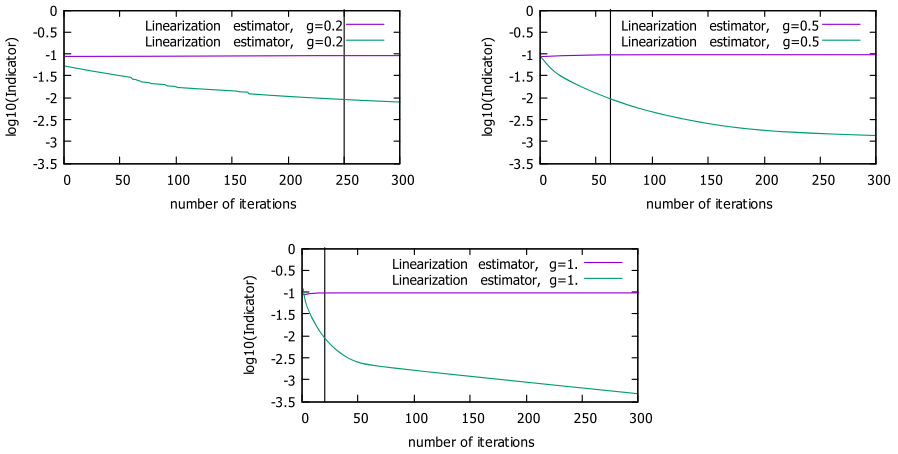


Fig. 3 The discretization and iteration indicators in logarithmic scale with respect to the number of iterations for $g = 0.2, 0.5, 1$. The vertical line indicates the iteration where the criterion (4.1) is reached for $\gamma = 0.1$

Algorithm 1 : Adaptive mesh strategy

Step 1 Given α_h^{n-1},

(a) Solve the problem (2.9) to compute $(\alpha_h^n, u_h^n, p_h^n)$.
(b) Calculate η_L^n and η_D^n.

Step 2 If the stopping criterion (4.1) is satisfied, go to Step 3, else set $\alpha_h^{n-1} = \alpha_h^n$ and go to Step 1.
Step 3

(a) If η_D^n is smaller than a fixed error tolerance ϵ, we stop the iterations and the algorithm.
(b) Else we adapt the mesh using the indicators $(\eta_{K,D}^n)$ given by (3.7).

Step 4 Set $n = n + 1$ and go to Step 1.

We note that the repartition of the finite element solution $\boldsymbol{u}_h^n$ depends on the external body forces $\boldsymbol{f}$.
Next, we introduce the relative total error indicator given as follows

$$E_{tot} = \frac{\eta_D^n}{\|\boldsymbol{u}_h^n\|_1 + \|p_h^n\|}$$

where η_D^n is computed after convergence on the iterations n (by using the stopping criteria (4.1)). Figure 6 shows and compares the relative total error indicator given by E_{tot} between the uniform and adaptive methods with respect to the total number of degrees of freedom. We mention here that E_{tot} represents the global indicator errors (while E_{err} in the previous case represents the total error between the exact and numerical solutions).

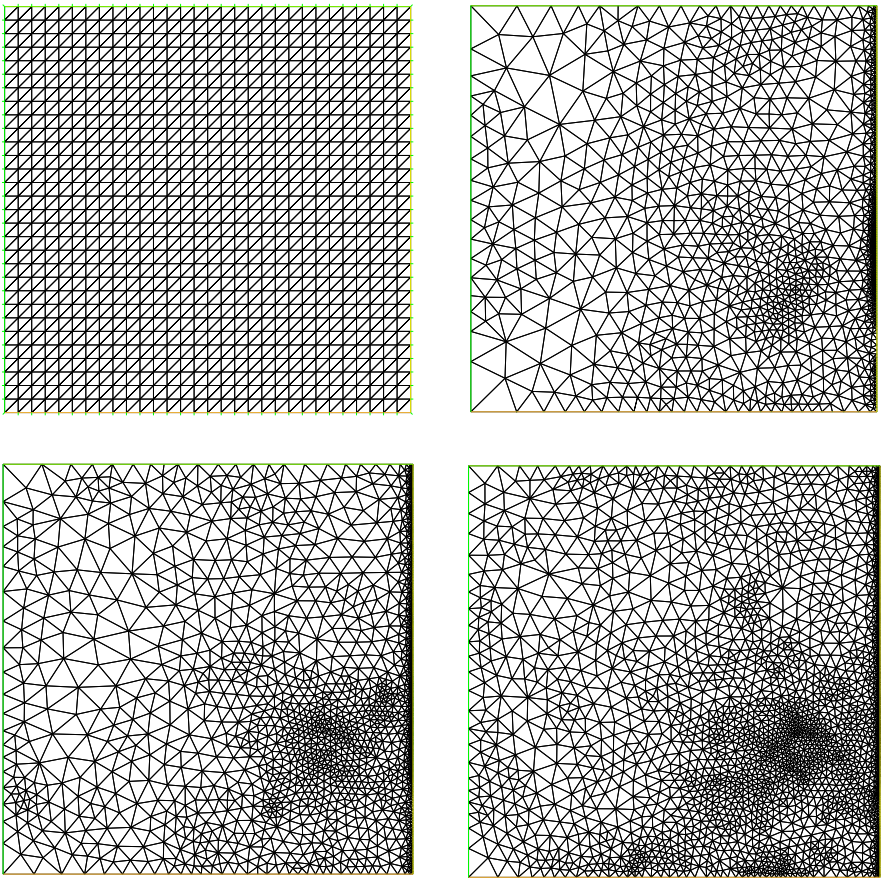


Fig. 4 Evolution of the mesh during the refinement levels (initial, first, second and third). We mention that the slip/stick condition (1.5) is located at the right part of the boundary $\partial\Omega$ corresponding to $x = 1$

In Table 1, we present the effectivity index defined as:

$$EI = \frac{\eta_D^n}{\|\boldsymbol{u} - \boldsymbol{u}_h^n||_1 + ||p - p_h^n||}$$

with respect to the number of vertices during the refinement levels. Here also η_D^n is computed after convergence on the iterations n and the exact solution $(\boldsymbol{u}, p)$ is approximated as described above. We remark that the values of EI for the considered case are between 5.40 and 5.57 which means that the effectivity index is bounded and more specifically it seems that it is constant in this case. Furthermore, Fig. 7 shows the error E_{tot} and the error

$$Ehn = (\|\boldsymbol{u} - \boldsymbol{u}_h^n||_1 + ||p - p_h^n||)/(\|\boldsymbol{u}_h^n||_1 + ||p_h^n||)$$

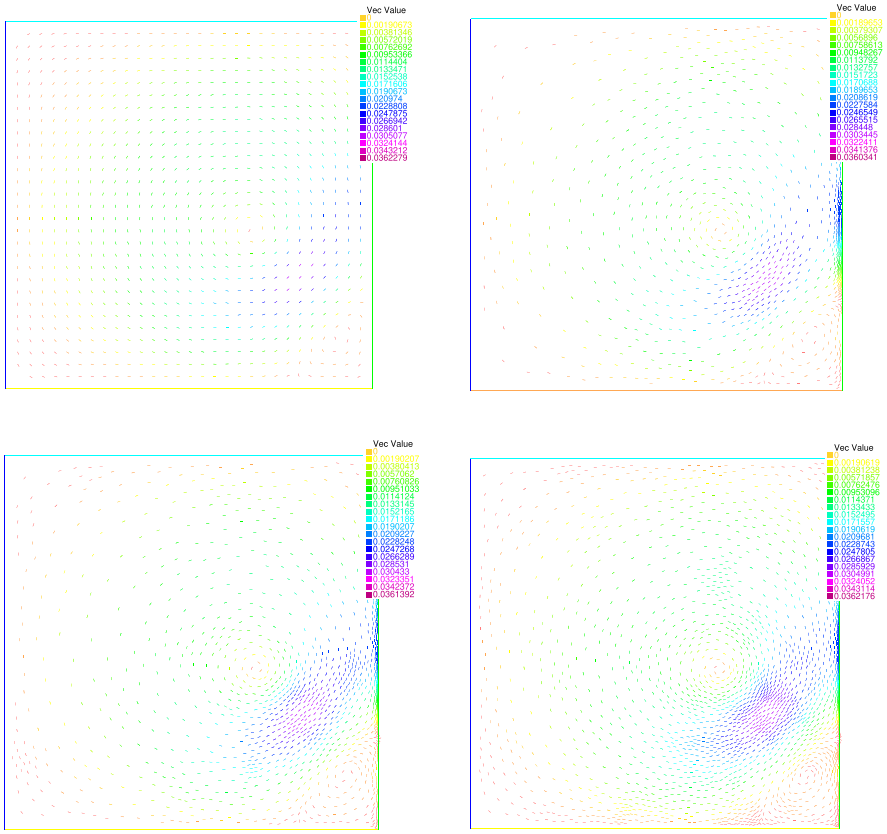


Fig. 5 Evolution of the velocity during the refinement levels (initial, first, second and third). The slip/stick condition (1.5) is located at the right part of the boundary $\partial\Omega$ corresponding to $x = 1$

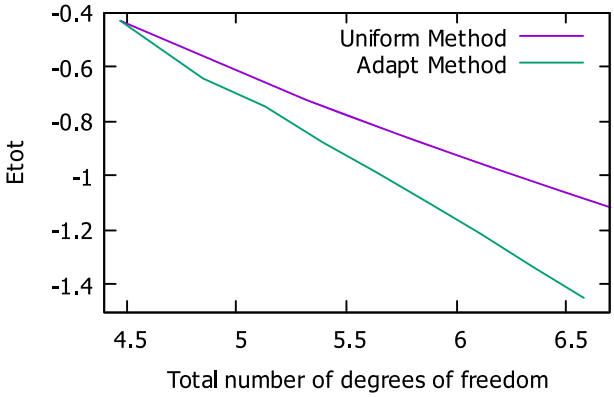


Fig. 6 Comparison of the errors E_{tot} with respect to the total number of degrees of freedom in logarithmic scale between the uniform and adaptive methods

Table 1 EI with respect to the refinement levels

Refinement level	First	Second	Third	Fourth	Fifth	Seventh	Eighth	Ninth
Number of vertices	70,864	136,872	246,864	434,280	748,392	1,288,472	2,212,648	3,804,408
Effectivity index	5.57	5.34	5.39	5.40	5.45	5.43	5.44	5.40

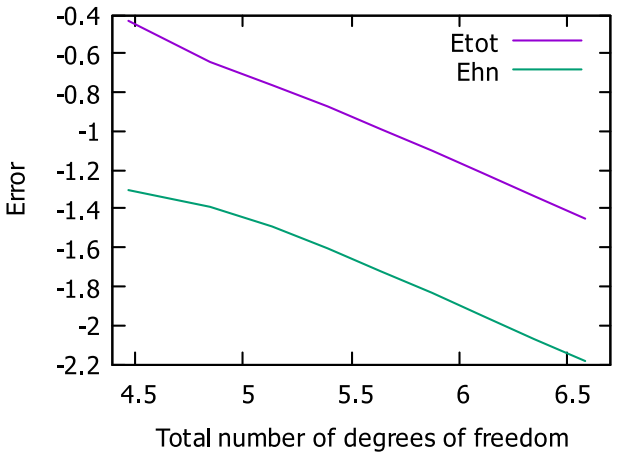


Fig. 7 Comparison of the errors E_{tot} and $Ehn = (\|\boldsymbol{u} - \boldsymbol{u}_h^n\|_1 + \|p - p_h^n\|)/(\|\boldsymbol{u}_h^n\|_1 + \|p_h^n\|)$ with respect to the total number of degrees of freedom in logarithmic scale

with respect to the total number of degrees of freedom in logarithmic scale. It seems that Table 1 and Fig. 7 give us the hope of the efficiency of the considered a posteriori error which will be the objective of a future work.

4.2 Example 2: lid driven cavity

This paragraph is devoted to the numerical solution for the lid driven cavity. This is very popular example that can be seen in several publications (see for instance [21, 55, 67, 68]). The fluid is confined in the domain $\Omega = (0, 1)^2$ and the boundary condition for the velocity field on the top is given by

$$\boldsymbol{u} = (16\, x^2(x-1)^2, 0)^T \quad \text{on} \quad y = 1 \quad 0 < x < 1.$$

Thus one has a smooth start of the flow, and the lid velocity attains its maximum, $\boldsymbol{u} = (1, 0)^T$, at the center $x = 1/2$. This boundary condition has the effect of avoiding local singularities at the top-right and top-left corners as it ensures both the velocity and velocity gradient vanish at the corners. On the other parts of $\partial\Omega$, we consider the boundary condition (1.5) in right part of the boundary corresponding to $x = 1$ and the homogeneous Dirichlet condition $\boldsymbol{u} = \boldsymbol{0}$ on the rest of $\partial\Omega$ ($x = 0$ and $y = 0$). In all the numerical results considered in this section, we set $g = 0.2$, $\rho = 0.2$, $\gamma = 0.05$ and $\nu = 0.5$.

Figure 8 show the evolution of the mesh during the refinement. We note that, for two consecutive iterations, the concentration of the refinement is on the complex vorticity regions and on the friction zone $S = \{(1, y)|$ and $0 \leq y \leq 1\}$. The distribution of the velocity in Ω is shown in Fig. 9. Finally, Fig. 10 shows a comparison of the error E_{tot} of the indicators between the uniform and the adaptive method. One can clearly observe the advantage of the adaptive method versus the uniform one.

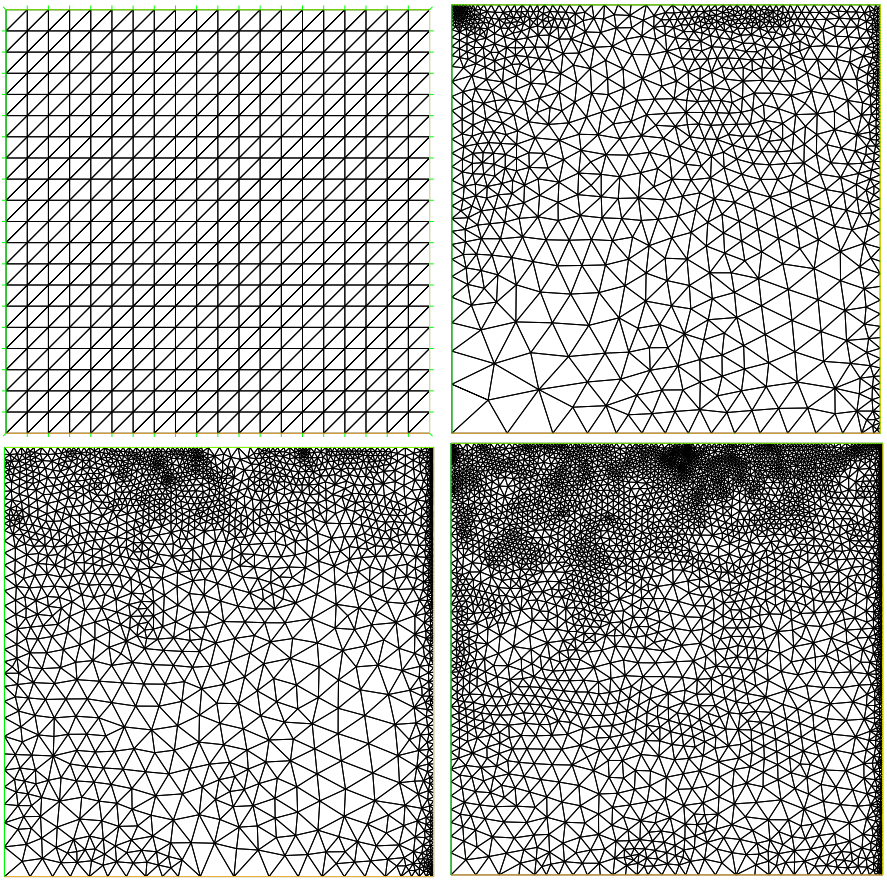


Fig. 8 Driven cavity: evolution of the mesh during the refinement levels (initial, first, second and third)

4.3 Concluding remarks

The objective of the present work is to propose a residual based a posteriori error estimate for the Stokes equations driven by Tresca boundary condition on one part of the boundary. The variational problem which is a variational inequality is first recast as a variational equation with the aid of Lagrange field computed via a projection operator. The finite element discretization of the problem is considered using the same procedure as the continuous formulation and the iterative solution based on Uzawa's approach is formulated. The main difference between this work and the previous ones is the fact that the error estimator is divided into two parts: discretization and linearization.

We prove the reliability by estimating the error bounds of the velocity and the pressure, but not the Lagrange field introduced earlier. The non consideration of the Lagrange field might be the origin of the lack of efficiency of the error estimator constructed. The numerical results obtained demonstrate the reliability of the posteriori

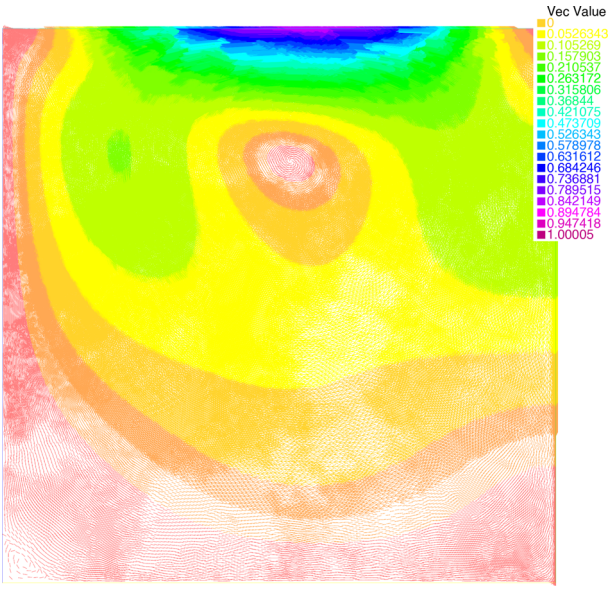


Fig. 9 Driven cavity: distribution of the velocity in the domain

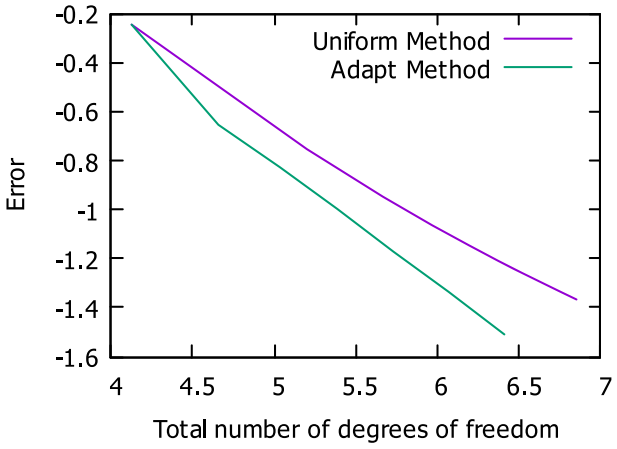


Fig. 10 Driven cavity: comparison of the errors E_{tot} with respect to the total number of degrees of freedom in logarithmic scale between the uniform and adapted methods

error estimate. The current methodology should be further developed, in particular by (i) considering time dependent problems (ii) extending the present analysis to quasi-variational and hemi-variational inequalities, (iii) incorporating the error on Lagrange field in the analysis and continuing with the investigation of the efficiency. An exploration of the close connection between Lagrange field technique suggested in [39] may provide a promising perspective of the present work.

Acknowledgements The authors thank the referees for their constructive remarks and comments.

Funding Not applicable.

Data availability statement Not applicable.

Declarations

Conflict of interest The authors declare no conflict of interest

Informed consent Not applicable.

References

1. Fujita. H.: A mathematical analysis of motions of viscous incompressible fluid under leak or slip boundary conditions. In: Mathematical Fluid Mechanics and Modeling, RIMS Kōkyūroko, Kyoto University, Kyoto, vol. 888, pp. 199–216 (1994)
2. Fujita, H.: A coherent analysis of Stokes flows under boundary conditions of friction type. J. Comput. Appl. Math. **149**, 57–69 (2002)
3. Le Roux, C.: Steady Stokes flows with threshold slip boundary conditions. Math. Models Methods Appl. Sci. **15**(8), 1141–1168 (2005)
4. Rajagopal, K.R.: On the implicit constitutive theories. Appl. Math. **48**(4), 279–319 (2003)
5. Shillor, M., Sofonea, M., Telega, J. J.: Models and Analysis of Quasistatic Contact: Variational Methods. Lect. Notes Phys., vol. 655, Springer, Berlin Heidelberg (2004)
6. Kikuchi, N., Oden, J.T.: Contact Problem in Elasticity. SIAM, Philadelphia (1988)
7. Duvaut, G., Lions, J.-L.: Inequalities in Mechanics and Physics. Grundlehren der Mathematischen Wissenschaften, vol. 219. Springer, Berlin (1976)
8. Glowinski, R., Lions, J.-L., Trémolières, R.: Numerical Analysis of Variational Inequalities. Studies in Mathematics and its Applications, vol. 8. North-Holland, Amsterdam (1981)
9. Falk, R.S.: Error estimates for approximations of a class of variational inequalities. Math. Comput. **28**, 963–971 (1974)
10. Brezzi, F., Hager, W.W., Raviart, P.A.: Error estimates for the finite element solution of variational inequalities. Numer. Math. **31**(4), 431–443 (1977)
11. Brezzi, F., Hager, W.W., Raviart, P.A.: Error estimates for the finite element solution of variational inequalities. II. Mixed methods. Numer. Math. **31**(1), 1–16 (1978)
12. Saito, N.: On the Stokes equations with the leak and slip boundary conditions of friction type: regularity of solutions. Publ. RIMS Kyoto Univ. **40**, 345–383 (2004)
13. Reddy, B.D.: Mixed variational inequalities arising in elastoplasticity. Nonlinear Anal. **19**(11), 1071–1089 (1992)
14. Han, W., Reddy, B.D.: On the finite element method for mixed variational inequalities arising in elastoplasticity. SIAM J. Numer. Anal. **32**, 1778–1807 (1995)
15. Brezis, H.: Functional Analysis, Sobolev Spaces and Partial Differential Equations. Springer, Berlin (2010)
16. Glowinski, R.: Numerical Methods for Nonlinear Variational Problems. Springer Series in Computational Physics. Springer, Berlin Heidelberg (2008)
17. Glowinski, R.: Finite element methods for incompressible viscous flow. In: Ciarlet, P.G., Lions, J.L. (eds.) Handbook of Numerical Analysis, vol. IX, pp. 3–1176. North Holland, Amsterdam (2003)
18. Ayadi, M., Gdoura, M.K., Sassi, T.: Mixed formulation for Stokes problem with Tresca friction. C.R. Acad. Sci. Paris Ser. I **348**, 1069–1072 (2010)
19. Ayadi, M., Baffico, L., Gdoura, M.K., Sassi, T.: Error estimates for Stokes problem with tresca friction conditions. Esaim: M2AN. **48**, 1413–1429 (2014)
20. Djoko, J.K., Koko, J.: GLS methods for Stokes equations under boundary condition of friction type: formulation-analysis-numerical schemes and simulations. SeMA. J. (2022). https://doi.org/10.1007/s40324-022-00312-2
21. Djoko, J.K., Koko, J.: Numerical methods for the Stokes and Navier–Stokes equations driven by threshold slip boundary conditions. Comput. Methods. Appl. Mech. Eng. **305**, 936–958 (2016)

22. Li, Y., Li, K.: Pressure projection stabilized finite element method for Navier–Stokes equations with nonlinear slip boundary conditions. Computing **87**, 113–133 (2010)
23. Kashiwabara, T.: On a finite element approximation of the Stokes equations under a slip boundary condition of the friction type. J. Ind. Appl. Math. **30**, 227–261 (2013)
24. Li, Y., Li, K.: Penalty finite element method for Stokes problem with nonlinear slip boundary conditions. Appl. Math. Comput. **204**, 216–226 (2008)
25. Haslinger, J., Stebel, J., Sassi, T.: Shape optimization for Stokes problem with threshold slip. Appl. Math. **59**(6), 631–652 (2014)
26. Gudi, T., Porwal, K.: A C^0 interior penalty method for a fourth order variational inequality of the second kind. Numer. Methods Partial Differ. Equ. **32**, 36–59 (2016)
27. Gudi, T., Porwal, K.: An a posteriori error estimator for a class of discontinuous Galerkin methods for Signorini problem. J. Comput. Appl. Math. **292**, 257–278 (2016)
28. Porwal, K.: Discontinuous Galerkin methods for a contact problem with Tresca friction arising in linear elasticity. Appl. Numer. Math. **112**, 182–202 (2017)
29. Braess, D., Carstensen, C., Ronald, H.W.: Convergence analysis of a conforming adaptive finite element method for an obstacle problem. Numer. Math. **107**(3), 455–471 (2007)
30. Chen, Z., Nochetto, R.H.: Residual type a posteriori error estimates for elliptic obstacle problems. Numer. Math. **84**, 4527–548 (2000)
31. Veeser, A.: Efficient and reliable a posteriori error estimates for elliptic obstacle problems. SIAM J. Numer. Anal. **39**, 146–167 (2001)
32. Wang, F., Han, W.: Another view for a posteriori error estimates for variational inequalities of the second kind. Appl. Numer. Math. **72**, 225–233 (2013)
33. Kornhuber, R.: A posteriori error estimators for the elliptic variational inequalities. Comput. Math. Appl. **31**, 49–60 (1996)
34. Bostan, V., Han, W.: Recovery-based error estimation and adaptive solution of elliptic variational inequalities of the second kind. Commun. Math. Sci. **2**, 1–18 (2004)
35. Bostan, V., Han, W., Reddy, B.: A posteriori error estimation and adaptive solution of elliptic variational inequalities of the second kind. Appl. Numer. Math. **52**, 13–38 (2004)
36. Bostan, V., Han, W.: A posteriori error analysis for finite element solutions of a frictional contact problem. Comput. Methods Appl. Mech. Eng. **195**, 1252–1274 (2006)
37. Xiao, W., Wang, F., Han, W.: Discontinuous Galerkin methods for solving a frictional contact problem with normal compliance. Numer. Funct. Anal. Opt. **39**, 1–17 (2018)
38. Wang, F., Ling, M., Han, W., Jing, F.: Adaptive discontinuous Galerkin methods for solving an incompressible Stokes flow problem with slip boundary condition of frictional type. J. Comput. Appl. Math. **371**, 112700 (2020)
39. Jing, F.F., Han, W., Zhang, Y.C., Yan, W.J.: Analysis of an aposteriori error estimator for a variational inequality governed by Stokes equations. J. Comput. Appl. Math. **372**, 112721 (2020)
40. Gustafsson, T., Lederer, P.L.: Mixed finite elements for Bigham flow in a pipe. Numer. Math. **152**(4), 819–80 (2022)
41. Braess, D.: A posteriori error estimators for obstacle problems-Another look. Numer. Math. **101**(4), 819–80 (2005)
42. Bürg, M., Schröder, A.: A posteriori error control of the hp-finite element for variational inequalities of the first and second kind. Comput. Math. Appl. **70**(12), 2783–2802 (2015)
43. Banz, L., Schröder, A.: A posteriori error control for variational inequalities with linear constraints in n abstract framework. J. Appl. Numer. Optim. **3**, 333–359 (2021)
44. Destuynder, P., Metivet, B.: Explicit error bounds in a conforming finite element method. Math. Comput. **68**, 1379–1896 (1999)
45. Braess, D., Schöberl, J.: Equilibrated residual error estimator for edge elements. Math. Comput. **77**, 651–672 (2008)
46. Dabaghi, J., Martin, V., Vohralík, M.: Adaptive Inexact semismooth newton methods for contact problem between two membranes. J. Sci. Comput. **84**(2), 28 (2020)
47. Dabaghi, J., Martin, V., Vohralík, M.: A posteriori estimates distinguishing the error components and adaptive stopping criteria for numerical approximations of parabolic variational inequalities. Comput. Methods. Appl. Mech. Eng. **367**, 113105 (2020)
48. Gharbia, B., Dabaghi, J., Martin, V., Vohralík, M.: A posteriori error estimates for a compositional two-phase flow with nonlinear complementarity constraints. Comput. Geosci. **24**, 1031–1055 (2020)

49. Gharbia, I.B., Ferzly, J., Volralík, M., Yousef, S.: Semismooth and smoothing newton methods for nonlinear systems with complementarity constraints: adaptivity and inexact resolution. J. Comput. Appl. Math. **133**(1), 12–29 (2023)
50. Gharbia, I.B., Ferzly, J., Vohralík, M., Yousef, S.: Adaptive inexact smoothing newton method for a nonconforming discretization of a variational inequality. Comput. Math. Appl. **133**, 12–29 (2023)
51. Chaillou, A.L., Suri, M.: Computable error estimators for the approximation of nonlinear problems by linearized models. Comput. Methods Appl. Mech. Eng. **196**, 210–224 (2006)
52. Chaillou, A.L., Suri, M.: Aposteriori estimators of the linearization error for strongly monotone nonlinear operators. Comput. Methods Appl. Mech. Eng. **205**, 72–87 (2007)
53. El Alaoui, L., Ern, A., Vohralík, M.: Guaranteed and robust a posteriori error estimate an balancing discretzation and linearization errors for monotone non linear problems. Comput. Methods. Appl. Mech. Eng. **200**, 2782–2795 (2011)
54. Bernardi, C., Dakroub, J., Mansour, G., Sayah, T.: A posteriori analysis of iterative algorithms for a nonlinear problem. J. Sci. Comput. **65**, 672–697 (2015)
55. Bernardi, C., Dakroub, J., Mansour, G., Sayah, T.: A posteriori analysis of iterative algorithms for Navier-Stokes problem. ESAIM: M2AN. **50**, 1035–1055 (2016)
56. Nassreddine, G., Omnes, P., Sayah, T.: A posteriori error estimates for the large eddy simulation applied to stationary Navier–Stokes equations. Numer. Methods Partial Differ. Equ. (2020). https://doi.org/10.1002/num.22850
57. Ciarlet, P.G.: The Finite Element Method for Elliptic Problems. Studies Math. Appl. North Holland, Netherland (1980)
58. Girault, V., Raviart, P.A.: Finite Element Methods for Navier–Stokes Equations: Theory and Algorithms. Springer, Berlin, Heidelberg, New-York, Tokyo (1986)
59. Girault, V., Wheeler, M.F.: Numerical discretization of a Darcy–Forchheimer model. Numer. Math. **110**, 161–198 (2008)
60. Scott, L.R., Zhang, S.: Finite element interpolation of nonsmooth functions satisfying boundary conditons. Math. Comput. **54**, 483–493 (1990)
61. Girault, V., Hecht, F.: Numerical methods for grade-two fluid models: finite-element discretizations and algorithms. In: Glowinski, R., Xu, J. (eds.) Handbook of Numerical Analysis, Numerical Methods for Non-Newtonian Fluids, vol. XVI, pp. 5–207. North Holland, Amsterdam (2011)
62. Verfürth, R.: A Posteriori Error Estimation Techniques For Finite Element Methods, Numerical Mathematics And Scientific Computation, Oxford (2013)
63. Evans, L.C., Gariepy, R.F.: Measure Theory and Fine Property of Functions. CRC Press, Boca Raton (1992)
64. Brenner, S.C., Ridgway, L.S.: The Mathematical Theory of Finite Element Methods, 3rd edn. Springer, Berlin (2010)
65. Hecht, F.: New development in FreeFem++. J. Numer. Math. **20**, 251–266 (2012)
66. Ern, A., Vohralík, M.: Adaptive inexact Newton methods with a posteriori stopping criteria for nonlinear diffusion PDEs. SIAMJ. Sci. Comput. **35**(4), A1761–A1791 (2013)
67. Owens, R.G.: Computational Rheology. Imperial College Press, London (2002)
68. Glowinski, R., Guidoboni, G., Pan, T.-W.: Wall-driven incompressible viscous flow in a two-dimensional semi-circular cavity. J. Comput. Phys. **216**, 76–91 (2006)

Publisher's Note Springer Nature remains neutral with regard to jurisdictional claims in published maps and institutional affiliations.

Springer Nature or its licensor (e.g. a society or other partner) holds exclusive rights to this article under a publishing agreement with the author(s) or other rightsholder(s); author self-archiving of the accepted manuscript version of this article is solely governed by the terms of such publishing agreement and applicable law.